THESIS

MEASUREMENT OF SNOWPACK PROPERTIES USING ACTIVE FM-CW MICROWAVE SYSTEMS

Submitted by

John Merritt Farr

Department of Earth Resources

In partial fulfillment of the requirements

for the Degree of Master of Science

Colorado State University

Fort Collins, Colorado

Summer, 1982

COLORADO STATE UNIVERSITY

JUNE 21 19 82

WE HEREBY RECOMMEND THAT THE THESIS PREPARED UNDER OUR SUPERVISION BY JOHN MERRITT FARR

ENTITLED MEASUREMENT OF SNOWPACK PROPERTIES USING ACTIVE FM-CW MICROWAVE SYSTEMS

BE ACCEPTED AS FULFILLING IN PART REQUIREMENTS FOR THE DEGREE OF MASTER OF SCIENCE

Committee on Graduate Work

James A. Smith

Norman W. Smith

H. S. Boyne

Adviser

H. S. Boyne

Department Head

ABSTRACT OF THESIS

MEASUREMENT OF SNOWPACK PROPERTIES

USING ACTIVE FM-CW MICROWAVE SYSTEMS

This paper reports on the use of an FM-CW active microwave system, in a research mode, to remotely sense water equivalence and liquid water content of snowpacks. A three-component "electrical path length" dielectric mixture model is described which accounts for the microwave system response as a function of operating frequency, snow density and depth (water equivalence), and liquid water content. This physically-based model is compared to currently accepted, semi-empirical mixture models and the limited data that exists. The electrical path length model compares favorably and has a distinctly simpler form than other models, making it workable for the specific problem addressed. It is concluded that by collecting data in two frequency ranges (just below the relaxation frequency of water), the depth of ice, the depth of liquid water, and thus the water equivalence of dry or wet snowpacks could be determined. Liquid water content determinations, made on a real-time basis, could then serve as invaluable melt-rate indexes for remote sites. Recommendations are given for the design configuration of an operational system, which could be incorporated into hydrometeorological data acquisition platforms such as SNOTEL.

John Merritt Farr
Earth Resources Department
Colorado State University
Fort Collins, Colorado 80523
Summer, 1982

ACKNOWLEDGEMENTS

I wish to express thanks to my advisor, Harold S. Boyne, for providing me with the research funds and guidance that made this work possible.

DEDICATED TO

Lottie Beer Horton

and

the memory of

Harold Merritt Horton

("Granny" and "Wog")

TABLE OF CONTENTS

LIST OF TABLES

LIST OF FIGURES

LIST OF SYMBOLS

$\bar{E}$ = electrical field intensity (newtons/meter)

WE = water equivalence of snow (cm)

T_w = water temperature (^oC)

α = attenuation constant (nepers/meter)

β = phase constant (radians/meter)

f = frequency (cycles/second or Hertz)

ω = angular frequency = $2\pi f$

μ_o = magnetic permeability of free space = $4\pi \times 10^{-7}$ Henrys/meter

μ = magnetic permeability = μ_o for non-magnetic media (snow)

ε = $\varepsilon' - i\varepsilon''$ = complex dielectric constant (farads/meter)

ε_o' = real part of free space dielectric constant = 8.854×10^{-12} F/m

ε_r' = relative dielectric constant = $\varepsilon'/\varepsilon_o'$ (dimensionless)

ε_s' = relative dielectric constant of wet or dry snow

ε_w' = relative dielectric constant of water

ε_i' = relative dielectric constant of ice

ε_a' = relative dielectric constant of air

c = speed of light = $1/\sqrt{\mu_o \varepsilon_o}$ = 2.99792×10^8 meters/second

v = velocity of propagation in dielectric media (meters/second)

ϕ = porosity of snow = $\theta + \theta_a$ (dimensionless)

θ = volumetric water content of snow (dimensionless)

θ_a = volumetric air content of snow (dimensionless)

ρ = free charge density (Coulombs/m^3)

ρ_s = density of snow (g/cm^3)

ρ_w = density of water = 1.0 g/cm^3

ρ_i = density of ice = 0.917 g/cm^3

d_{fs} = depth of free space (cm) - see figure 3

d_i = depth of ice (cm)

d_w = depth of water (cm)

d_a = depth of air (cm)

d_s = depth of snow = $d_i + d_a + d_w$ (cm)

Debye equation parameters (figure 1):

ε'_{ro} = static relative dielectric constant, a function of both dipolar and electronic polarization processes.

$\varepsilon'_{r\infty}$ = high frequency relative dielectric constant, a function of electronic polarization only.

f_m = relaxation frequency of the media, where loss tangent is a maximum.

Mixing formulas (table 2):

V_i = volume fraction of ice, V_w = volume fraction of water

A_{kj} = polarization factors for ice (k=i) and water (k=w)

ε_{ws} = relative dielectric constant of wet snow = ε'_s in thesis text

CHAPTER I

INTRODUCTION

1.1 Water Supply and Flood Forecasting Needs

Both long and short term snowmelt-runoff forecasts are dependent upon accurate and timely information on snowpack water equivalence, precipitation rates, and melting rates. These data requirements have spurred the development of automated remote data acquisition networks, such as the Soil Conservation Service SNOTEL System. The standard SNOTEL data acquisition platform consists of an array of snow pillows, a shielded storage precipitation gage, and an air temperature sensor. Snow pillows sense snowpack water equivalence indirectly by measuring the downward forces transmitted to the pillows by overlying snow. It would be preferable to employ a device which more directly measures the water equivalence instead of the transmitted forces of a snowpack (Smith and Boyne, 1982). The problems associated with precipitation gage measurement of snowfall are numerous and well documented (Goodison, et. al., 1981). Although the data from SNOTEL is excellent, problems do exist such as "bridging" over snow pillows and "capping" of precipitation gages (Shafer, 1980). Both of these shortcomings cause problems in the spring, when data accuracy is most critical. In addition, the only reliable melt-rate index SNOTEL provides is air temperature. Snow pillow data must be used with caution in this regard, because the pillows do not always respond properly to unweighting, and sublimation

losses are hard to account for. Thus, data of a more accurate nature is still needed for runoff forecasting, and the designers of the SNOTEL data telemetry system provided additional transmission channels to carry such data.

1.2 Avalanche Forecasting Needs

Avalanche forecasting has some similar data requirements. The quantity or water equivalence of snow and the loading rates (precipitation plus wind-transported snow) in avalanche starting zones induce the stresses which lead to failure or release. High liquid water contents cause intergranular bonds to melt, leading to wet-snow avalanches (Perla and Martinelli, 1976). The starting zones in avalanche country are difficult, if not dangerous to access, and remote data collection tools applicable to this problem are limited.

1.3 Objective and Methods of Investigation

The FM-CW (frequency modulated-continuous wave) microwave system described in this paper and similar active microwave systems have potential for satisfying some of the above mentioned data requirements. This paper strives to develop further the relevant technology necessary to remotely sense snow (especially wet snow) with active microwave systems such as the FM-CW.

To this end, a dielectric mixture model is presented which relates the hydrologic properties of the snowpack (snow depth, density, and liquid water content) to the electrical properties of the snowpack. These electrical properties govern electromagnetic wave velocities, and the response of the FM-CW is, in part, a measure of these velocities.

Thus, with the aid of the dielectric mixture model, the FM-CW response gives a measure of the hydrologic properties of the snowpack.

In addition to developing this dielectric mixture model, measurements were made in the lab and the field in an attempt to confirm the utility of the mixture model for use with FM-CW data. The model is also compared to other models and data available from previous investigations.

1.4 Previous Investigations

Previous investigations have included data collection (Ambach and Denoth, 1972; Boyne and Ellerbruch, 1980; Cumming, 1952; Linlor, et. al., 1980; Sweeny and Colbeck, 1974; Tobarias, et. al., 1978; Vickers and Rose, 1973), dielectric modelling (Colbeck, 1980; Ellerbruch and Boyne, 1980; Looyenga, 1965; Polder and Van Santen, 1946; Sweeny and Colbeck, 1974; Tinga and Voss, 1973; Wiener, 1910), and regression analysis (Linlor, et. al., 1980). Just as in this present work, some of the above investigations involved comparing models with other models and/or data. Chapter III (Comparison of Electrical Path Length Model) elaborates further on these previous investigations.

CHAPTER II

ELECTRICAL PATH LENGTH DIELECTRIC MIXTURE MODEL

2.1 Background Electromagnetic Theory

Maxwell's field equations, equations (1) through (4) below, describe the relations between spatial and temporal variations in electromagnetic field intensities, charge distribution, and host-medium electrical properties.

$$\nabla \times \overline{H} = \overline{J} + \frac{\partial \overline{D}}{\partial t} \tag{1}$$

$$\nabla \times \overline{E} = -\frac{\partial B}{\partial t} \tag{2}$$

$$\nabla \cdot \overline{D} = \rho \tag{3}$$

$$\nabla \cdot \overline{B} = 0 \tag{4}$$

The following auxilary definitions relate field intensities and fluxes to the medium properties (σ, ε, μ)[1]

$$\overline{J} = \sigma\overline{E} \quad \text{(conduction flux density - } A/m^2\text{)} \tag{5}$$

$$\overline{D} = \varepsilon\overline{E} \quad \text{(displacement flux density - } A/m^2\text{)} \tag{6}$$

$$\overline{B} = \mu\overline{H} \quad \text{(magnetic flux density - } Wb/m^2\text{)} \tag{7}$$

where $\overline{E}$ is electric field intensity (N/C) and $\overline{H}$ is magnetic field intensity (A/m). Using the auxiliary definitions above, Maxwell's equations can

---

[1]See list of symbols for definition of terms.

be solved to yield an expression for $\overline{E}$ in terms of time and space for plane electromagnetic waves propagating in a general medium (Johnk, 1975):

$$\overline{E}_x = \overline{E}_{ox}\, e^{-\alpha z} \cos(\omega t - \beta z) \qquad (8)$$

This is for an x-polarized wave travelling in the z-direction (vertically), where $\overline{E}_{ox}$ is the peak amplitude of the wave, α is the attenuation constant, β is the phase constant, ω is the angular frequency, and t is time.

Equation (8) is obtained under the assumptions that:

1. The vector components of $\overline{E}$ and $\overline{H}$ do not vary with x or y; i.e., $\partial/\partial x = \partial/\partial y = 0$ for all field components.
2. The free charge densities are zero throughout the medium ($\rho = 0$), but a conduction flux density can exist which is related to the $\overline{E}$ field by equation (5), $\overline{J} = \sigma\overline{E}$.
3. The bulk electrical properties of the medium (μ, ε, σ)[1] are assumed linear, homogeneous and isotropic.

So long as the FM-CW radar antennas are sufficiently distant from the snow surface (greater than approximately one meter, depending on the type of antennas), assumption number one above is quite justified. Assumption two is of no concern in a natural snowpack. The magnetic permeability μ of snow is the same as that of free space (a constant μ_o), and thus we need not be concerned with it at all in assumption number three. The dielectric constant ε and conductivity σ of snow are both linear

---

[1] See list of symbols for definition of terms.

with respect to electric and magnetic polarization effects. The homogeneity and isotropy of ε and σ will be discussed in subsection "Examination of Model Assumptions" later in this chapter.

2.1.1 Velocity of Propagation

It is evident that if equation (8) were to describe the motion of a wave crest (where $\overline{E}_x = \overline{E}_{ox}e^{-\alpha z}$), $\omega t = \beta z$ must hold and the velocity of propagation is

$$v = z/t = \omega/\beta \tag{9}$$

The phase constant for a lossy dielectric[1] is (Johnk, 1975)

$$\beta = \frac{\omega\sqrt{\mu\varepsilon'}}{\sqrt{2}}\left[\sqrt{1 + \left(\frac{\varepsilon''}{\varepsilon'}\right)^2} + 1\right]^{\frac{1}{2}} \tag{10}$$

where the imaginary part of the complex dielectric constant ε'' is descriptive of <u>all</u> loss mechanisms operating in the medium at a given frequency (Johnk, 1975, p. 173). This implies that if conductivity plays a significant role in the losses of the medium, it must be included in the ε'' term. This can be done with the use of an "effective loss term"

$$\varepsilon''_{eff} = \varepsilon'' + \frac{\sigma}{\omega} \tag{11}$$

An alternate form of equation (10), preferred for use describing a conductive medium, is

$$\beta = \frac{\omega\sqrt{\mu\varepsilon'}}{\sqrt{2}}\left[\sqrt{1 + \left(\frac{\sigma}{\omega\varepsilon'}\right)^2} + 1\right]^{\frac{1}{2}} \tag{12}$$

---

[1] See list of symbols for definition of terms.

If equation (12) is applied to a conductive medium with significant dielectric losses, this can be taken into account with

$$\sigma_{eff} = \sigma + \omega\varepsilon'' \tag{13}$$

It can be seen that the loss tangent can be defined as either $\varepsilon''/\varepsilon'$ or $\sigma/\omega\varepsilon'$ (equations 10 or 12) depending upon the dominant loss mechanism and the preference of the user (see Appendix A for a discussion of dielectric relaxation and dielectric loss).

In the microwave region of the electromagnetic spectrum, water is a very lossy dielectric (i.e., the imaginary part of the complex dielectric constant ε'' is large, see Figure 1c and Appendix A). Thus, the form of the phase constant given in equation (10) would need to be used unmodified to describe propagation velocities in liquid water. However, the existing data for wet snow indicate that the loss tangent ($\varepsilon''/\varepsilon'$) would be less than 0.2 for liquid water contents up to 8% by volume and operating frequencies up to 6 GHz. This liquid water content limit of 8% by volume converts to a range of approximately 16% - 27% by weight, depending on snow density, which covers the range normally encountered in a freely draining snowpack. However, this liquid water content limit would be exceeded when slush layers develop above flow impediments such as ice lenses or saturated soil. Under the above restrictions, $\varepsilon''/\varepsilon'$ would be small enough to be neglected from equation (10), leaving

$$\beta = \omega\sqrt{\mu\varepsilon'} \tag{14}$$

With the use of equation (9), the velocity of propagation becomes

$$v = 1/\sqrt{\mu\varepsilon'} \tag{15}$$

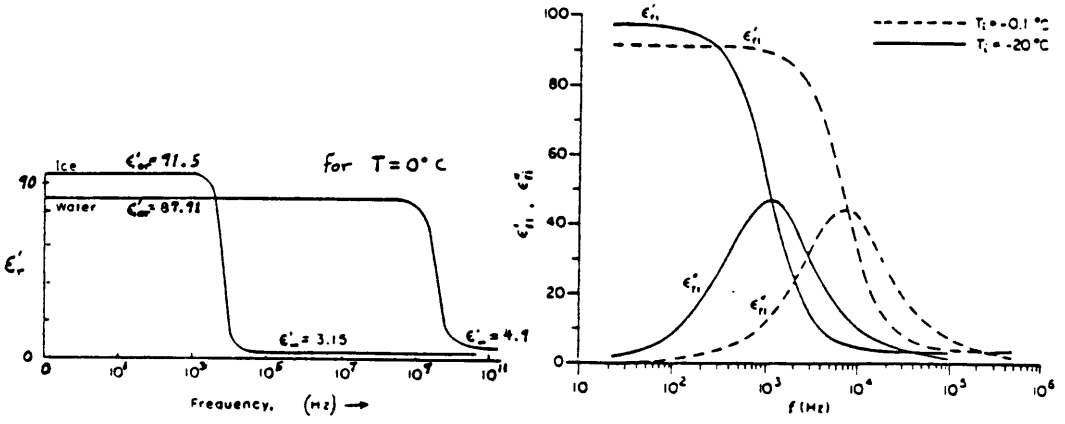

(a) *Dielectric relaxation of ice and water occur at widely different frequencies.*

(b) *Relative permittivity of ice at low frequencies.*

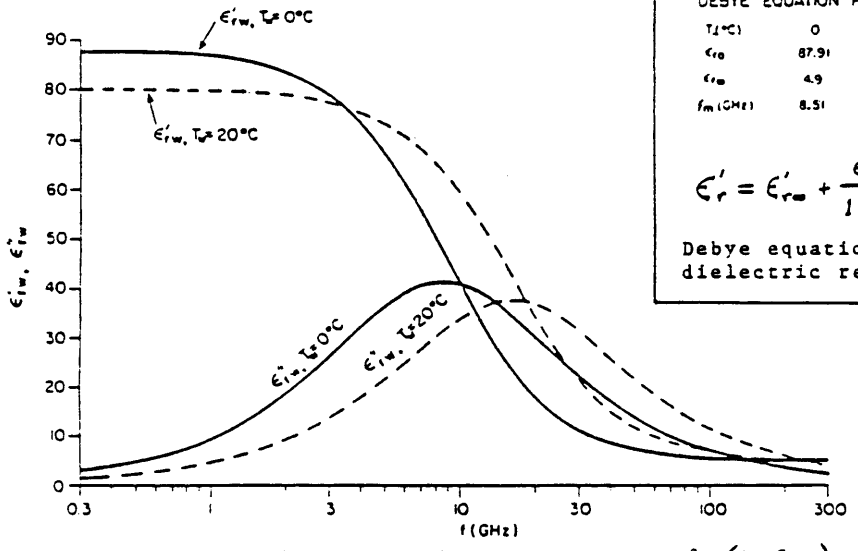

DEBYE EQUATION PARAMETERS

T_i (°C)	0	20
ϵ'_{r0}	87.91	80.21
$\epsilon'_{r\infty}$	4.9	4.9
f_m (GHz)	8.51	15.76

$$\epsilon'_r = \epsilon'_{r\infty} + \frac{\epsilon'_{r0} - \epsilon'_{r\infty}}{1 + (f/f_m)^2}$$

Debye equation of dielectric relaxation

(c) *Relative permittivity of water at T_w = 0°C (Wet Snow) and T_w = 20°C using the Debye equation.*

Figure 1. Relative dielectric constants of ice and water, showing the associated dielectric relaxations (from Royer, 1973).

Unless the snow is dirty (i.e., with significant conduction losses, see Appendix A), the error associated with the above simplification, under the stated water content and frequency restrictions, would not be greater than 0.5%, and in most cases much less than that. Using the free-space propagation velocity $c = 1/\sqrt{\mu_0 \varepsilon_0'}$, equation (15) can be written in terms of the relative dielectric constant of the medium $(\varepsilon_r' = \varepsilon'/\varepsilon_0')$ as

$$v = c/\sqrt{\varepsilon_r'} \qquad (16)$$

2.2 Mixture Model Description in Relation to FM-CW

The FM-CW used in this work is a sweep-frequency radar operating in the 2-8 GHz range. The sweep rate was generally 50-100 sweeps per second. Another FM-CW, operating at 8-12.4 GHz, broke down before any conclusive data could be obtained with it. Thus, data has only been collected in the 2-8 GHz range. The FM-CW operation is schematically depicted in Figure 2, and a detailed description can be found in the Manual of Remote Sensing, American Society of Photogrammetry, 1975. FM-CW radars of the type described here have been used previously to measure coal layer thickness and water equivalence of dry snowpacks (Ellerbruch and Belsher, 1978; Ellerbruch and Boyne, 1980). The main advantage of an FM-CW over a pulse radar is the improved range resolution. However, a pulse radar would perform suitably as long as the pulse width was on the order of 10^{-9} seconds or less (see Vickers and Rose, 1973, for a discussion of their nanosecond pulse width radar). In fact, there may be some advantages to a pulse radar vs an FM-CW when dealing with a frequency dependent dielectric medium such as wet snow. This will be mentioned again in Chapter V.

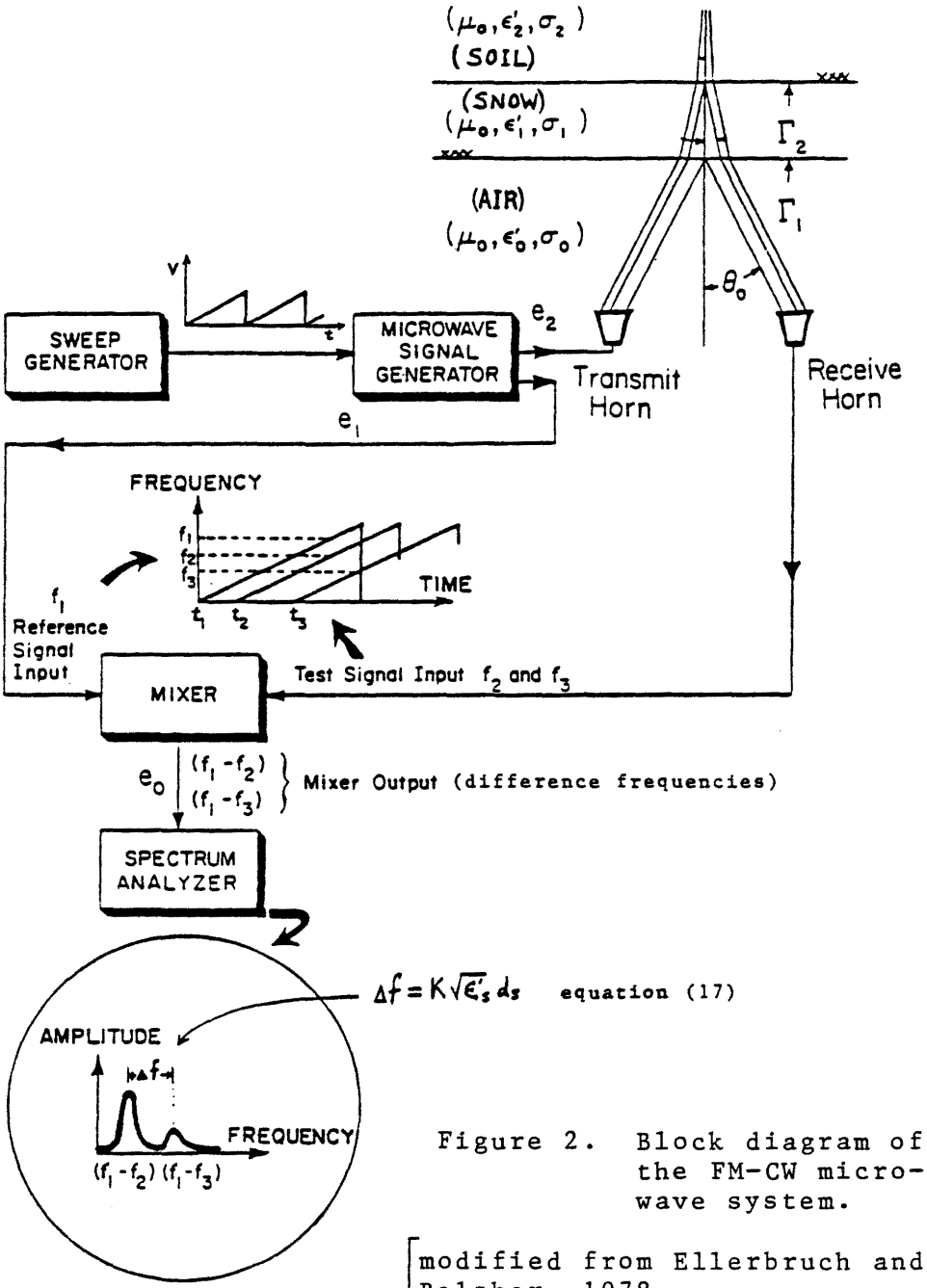

Figure 2. Block diagram of the FM-CW microwave system.

[modified from Ellerbruch and Belsher, 1978]

The dielectric constants of ice and air (components 1 and 2 of the wet snow mixture) are frequency independent throughout the microwave region, and are taken to be $\varepsilon_i' = 3.15$ and $\varepsilon_a' = 1.0$ respectively. On the other hand, the dielectric constant (or permittivity) of water is a function of frequency in this region (Figure 1), and because the FM-CW sweeps over 2-8 GHz, the system response is an average response to the dielectric properties over the sweep band. Thus, the relative dielectric constant to be used interpreting data collected in this frequency range is obtained by integrating the Debye equation, given in Figure 1, from 2-8 GHz (for $T_w = 0^oC$) and dividing the result by the sweep bandwidth (6 GHz). This gives $\varepsilon_w' = 66.56$ and will be denoted $\varepsilon_{w(2-8)}' = 66.56$. The dielectric properties of these three components will be mixed, using the dielectric mixture model, to get the relative dielectric constant of the snowpack.

The output of the FM-CW is a plot on the spectrum analyzer of relative amplitude vs mixer difference frequencies. These difference frequencies are simply functions of the two-way propagation times from the radar to dielectric discontinuities. The return signals are referenced internally against the transmitted signal to get a difference frequency corresponding to each dielectric discontinuity, as shown in Figure 2. The electrical path length $\sqrt{\varepsilon_s'}d_s$ is proportional to a displacement frequency measure Δf between the air/snow and snow/soil discontinuities

$$\Delta f = K\sqrt{\varepsilon_s'}d_s \tag{17}$$

where $K = 2(f_2 - f_1)f_n/c$ = system constant, $(f_2 - f_1)$ is the sweep bandwidth, f_n is the number of sweeps per second, c is the speed of light,

d_s is the physical depth of the snowpack, and ε_s' is the relative dielectric constant of the snow. To provide some physical meaning, the electrical path length ($\sqrt{\varepsilon_s'}d_s$) can be defined as the distance separating dielectric discontinuities in free space that would give the same displacement measurement as that obtained from discontinuities separated a distance d_s in the dielectric medium. Equation (17) incorporates the simplification made in deriving equation (14), thus the medium under observation must fit the criteria of a good dielectric (i.e., the loss tangent must be small).

The electrical path length of the snow mixture $\sqrt{\varepsilon_s'}d_s$ can be written in terms of its components[1] as (see Figure 3)

$$\sqrt{\varepsilon_s'}d_s = \sqrt{\varepsilon_i'}d_i + \sqrt{\varepsilon_a'}d_a + \sqrt{\varepsilon_w'}d_w \tag{18}$$

Since $\varepsilon_a' = 1.0$, equation (18) can be written as

$$\sqrt{\varepsilon_s'}d_s = \sqrt{\varepsilon_i'}d_i + d_a + \sqrt{\varepsilon_w'}d_w \tag{19}$$

Because $d_s = d_i + d_a + d_w$ and $\varepsilon_i' = 3.15$, equation (19) can be written as

$$\sqrt{\varepsilon_s'}d_s = 1.775d_i + d_s - (d_i + d_w) + \sqrt{\varepsilon_w'}d_w \tag{20}$$

These equations constitute the electrical path length dielectric mixture model. Much credit is due to Ellerbruch and Boyne, 1980, for this model, which is simply an extension of their 2-component (ice and air) model to allow for the presence of liquid water.

---

[1] See list of symbols for definition of terms

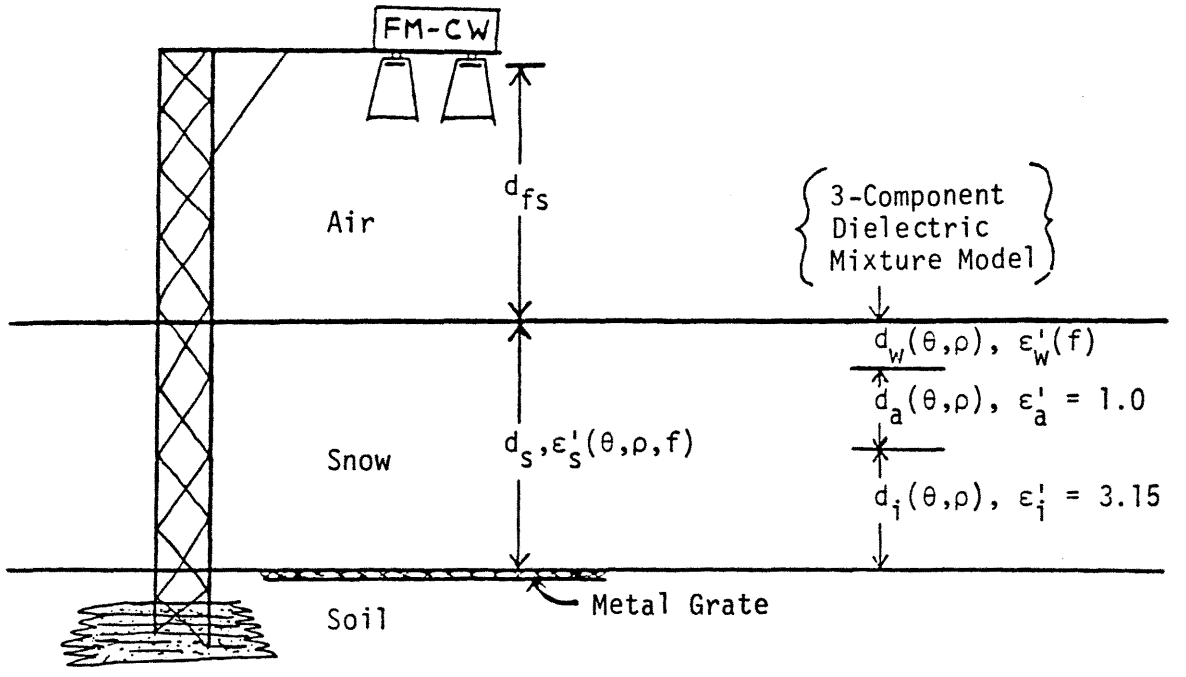

Figure 3. Hypothetical Design Configuration for FM-CW in a hydrometeorological data acquisition platform. Also shown is a schematic representation of the electrical path length dielectric mixture model of the snowpack.

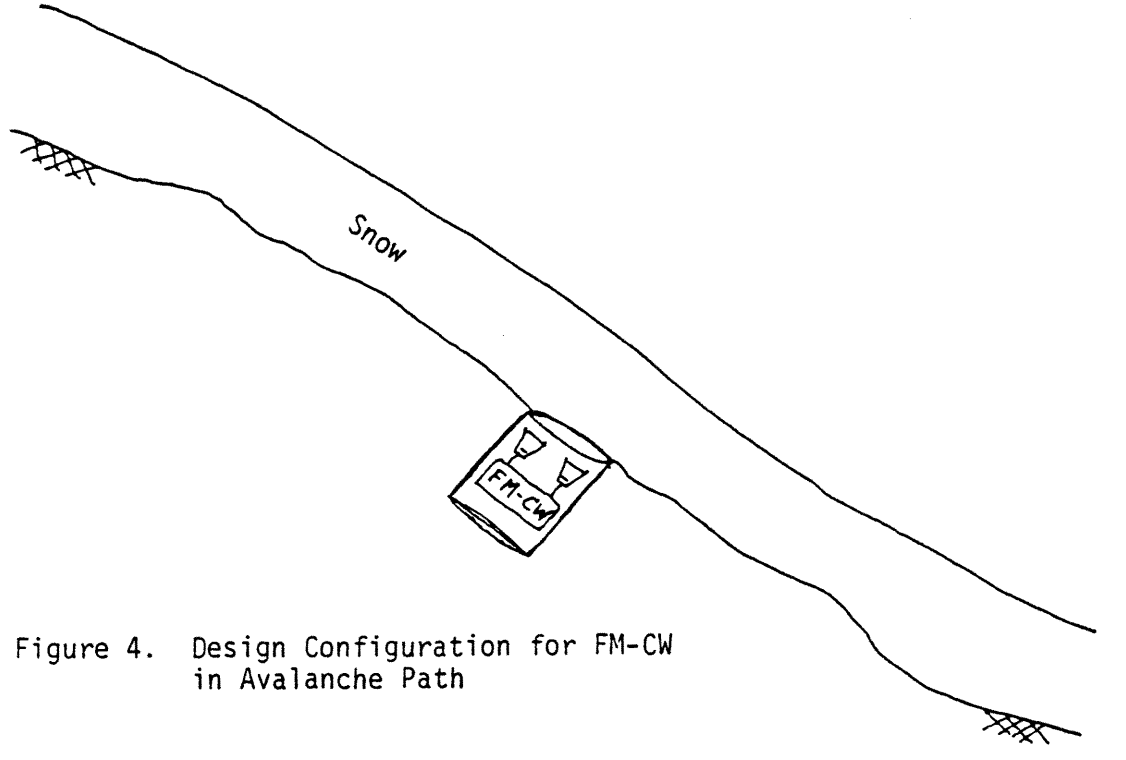

Figure 4. Design Configuration for FM-CW in Avalanche Path

2.3 Examination of Model Assumptions

As shown in Figure 3, this model assumes that the depths of each component (ice, air, and water) through which radiation propagates vertically will be in the same proportions as these components occur on a volumetric basis. The snow mixture is treated as if it were block-wise homogeneous; i.e., the three components of the mixture are lumped into layers, each of which can itself be considered dielectrically homogeneous. For example, in the case of dry snow, porosity defined on a vertical line is assumed numerically equivalent to the volumetric porosity. As long as the ice grains are randomly distributed with no preferential orientation in space, this assumption (with respect to the ice) is perfectly sound, especially considering the spatial averaging taking place as a result of the large "footprint" (area of electromagnetic sampling, a result of spreading of radiation from antenna). The only time this might not apply would be when observing a layer of depth hoar snow crystals, which grow by vapor diffusion in the presence of large thermal gradients (Sommerfeld and LaChapelle, 1970). These large faceted grains are well oriented on the macroscopic scale due to vertically upward migration of vapor along the thermal gradient. Internally, the c-axes of the crystal lattice show a very strong tendency to line up vertically. This last condition may induce a slight dielectric anisotropy in relation to low frequencies (< 10 kHz), but at microwave frequencies, ice can be considered isotropic. Measurements of the static dielectric constant made on single ice crystals showed anisotropy to be about 14%, with the dielectric constant measured along the c-axis

greater than that measured in the basal plane (Fletcher, 1970, p. 201). Thus, if it were desired to develop an electromagnetic device capable of detecting depth hoar (for use in avalanche forecasting), it would have to operate at low frequency and be extremely accurate in order to discern any dielectric anisotropy.

With respect to the liquid water inclusions, the proportioning of electrical path lengths volumetrically would be acceptable to the extent that these inclusions were randomly distributed/oriented in space. This should be the case as long as capillary forces predominate over gravitational forces in controlling the orientation of the air/water interfaces and thus the orientation of the liquid water inclusions. Again, considering the spatial averaging taking place over the footprint, this assumption seems plausible over the grain sizes and liquid water contents commonly encountered. During very rapid snowmelt, when solution channels sometimes develop and water contents are very high, this assumption may break down, but more importantly, the snow becomes a lossy dielectric, invalidating equation (16).

CHAPTER III

COMPARISON OF ELECTRICAL PATH LENGTH MODEL

To the extent that the simplification of equation (10) and other assumptions are valid, the dielectric mixture model presented here can be used to predict what the dielectric constant of various snow mixtures should be. Knowing the ground truth values of snow density and liquid water content, the dielectric constant of snow as a function of frequency can be predicted. The values so derived can be compared to actual measurements and values predicted by other mixture models.

3.1 Data Collection

In this study, data was collected in both field and laboratory settings. All of the snow sampled was of the equi-temperature or melt-freeze type (see Sommerfeld and LaChapelle, 1970). The laboratory was a walk-in cold room at the Forest Service Rocky Mountain Forest and Range Experiment Station in Fort Collins, Colorado. Snow samples gathered in the mountains west of Fort Collins were placed into an open Plexiglas box, measuring approximately 62 cm by 62 cm in the plane perpendicular to the microwave beam and 20 cm deep. A metal plate was placed on the bottom of the box, under the snow sample, to provide a strong return signal (large dielectric discontinuity). The temperature was kept constant (plus or minus 1^{o} C) at -2^{o} C for a couple of days prior to sampling in order to promote equi-temperature metamorphism (Sommerfeld and LaChapelle,

1970). Snowmelt was induced by raising the cold room temperature well above freezing until a desired level of snow wetness was achieved. The temperature was then lowered to 0^{o} C during microwave and ground truth measurement.

The FM-CW was suspended approximately 120 cm above the snow sample on a crossbar between two tripods. As microwave data was obtained, the snow density, depth, and liquid water content were determined. The density was measured with a LaChapelle density kit, and the liquid water content was determined using cold calorimetry (see Jones, et. al., 1980 for details of this technique). The data points of 3-11-82 and 3-4-82 (Table 1) were collected in the laboratory in this manner.

The field data was collected at the Joe Wright SNOTEL site on Cameron Pass, west of Fort Collins. Measurements were carried out in the natural snowpack overlying a metal snow pillow, in much the same manner as described above except that because of the greater snow depth, a complete density profile was taken and liquid water contents were determined at multiple heights above the ground surface. Figure 5 shows the ground truth field data in the form of snow profiles (see Perla and Martinelli, 1976 for a key to the international symbols used). Figure 6 is an example of the FM-CW system output, a permanent trace of the spectrum analyzer display which was made on an x-y plotter in the field. Both of the field dates (5-2-81 and 5-14-81) were after the snowpack had become isothermal and no significant impediments to percolating melt water (ice lenses) remained. The snowpack profile consisted of fairly homogeneous equi-temperature and melt-freeze grains with some grain size variations. Layers of uniform wetness were visually discerned, and cold calorimetry samples were taken from each of these layers (Figure 5). The

TABLE 1

FM-CW Data [$\varepsilon'_{w(2-8)} = 66.56$]

Date	Water Content (θ)	Porosity (ϕ)	Elect. Path Length Model Predicted Values (ε'_{sp})	Measured Values (ε'_{sm})	Squared Error ε'_{sp} vs ε'_{sm} (SE)	Relative Error (RE)	Imaginary Part of Diel. Const. (ε''_{sm})
3-11-82	0.0263	0.5598	2.34	2.14	0.0040	0.0935	-
3-11-82	0.0428	0.5778	2.67	2.83	0.0256	-0.0565	-
3-4-82	0.0355	0.6134	2.41	2.54	0.0169	-0.0512	-
3-4-82	0.0450	0.6238	2.60	2.73	0.0169	-0.0476	-
5-2-81	0.0345	0.6592	2.28	2.11	0.0289	0.0806	-
5-14-81	0.0404	0.6656	2.40	2.26	0.0196	0.0619	-
					MSE = 0.0247	MRE = 0.0134	

Sweeny & Colbeck's Data (1974) $\varepsilon'_{w6} = 60.35$

θ	ϕ	ε'_{sp}	ε'_{sm}	SE	RE	ε''_{sm}
0.0548	0.3874	3.41	4.13	0.5184	-0.1743	0.80
0.0980	0.3420	4.72	5.13	0.1681	-0.0799	1.23
0.0506	0.3195	3.50	4.61	1.2321	-0.2408	0.89
0.0696	0.3807	3.81	3.33	0.2304	0.1441	0.41
0.0980	0.2934	4.89	5.45	0.3136	-0.1028	1.76
0.0703	0.3232	4.00	3.63	0.1369	0.1019	0.55
0.0485	0.3448	3.37	3.27	0.0100	0.0306	0.35
0.0482	0.2942	3.51	3.34	0.0289	0.0509	0.42
0.1065	0.3286	5.02	4.39	0.3969	0.1435	0.95
0	0.3660	2.22	2.19	0.0009	0.0137	0.003
				MSE = 0.3036	MRE = -0.0113	

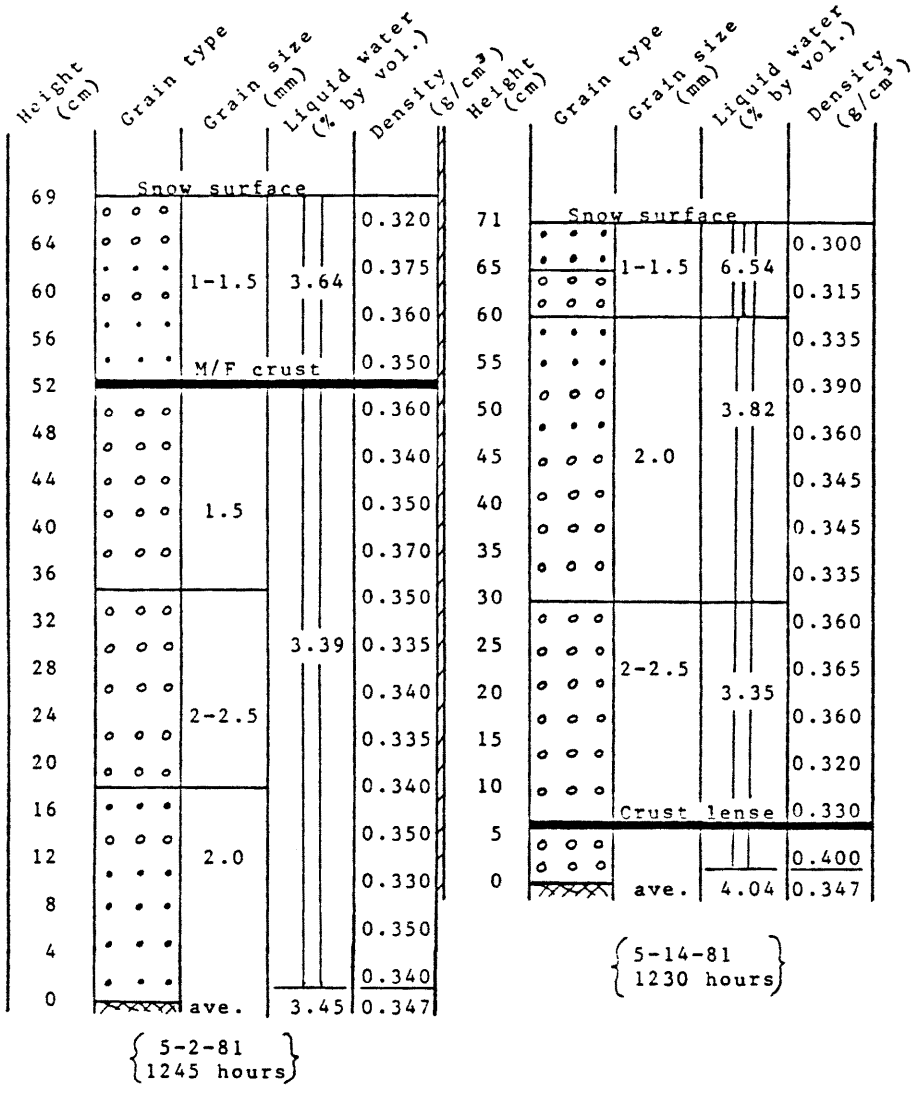

Figure 5. Field data snow profiles from Joe Wright SNOTEL site.

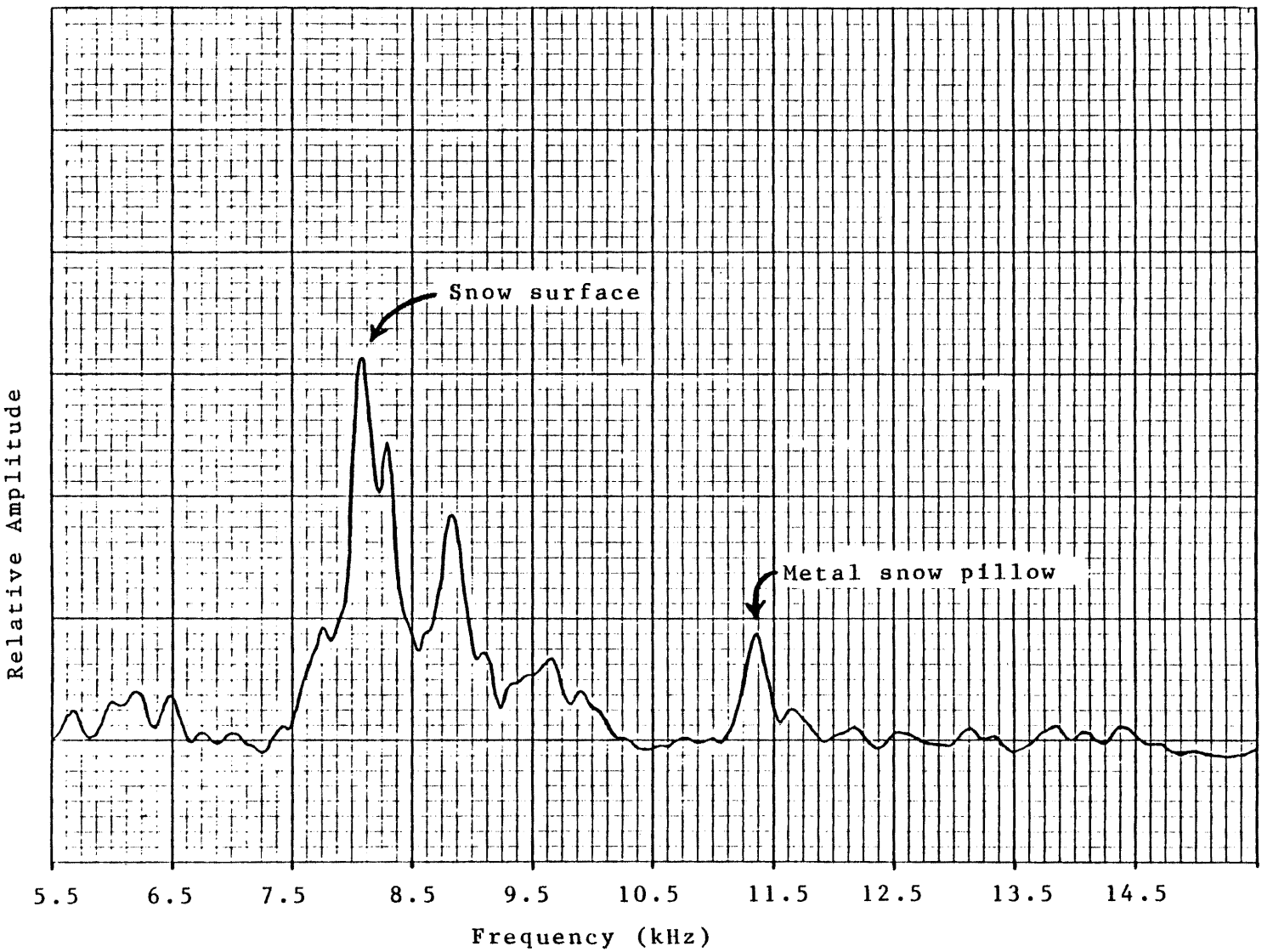

Figure 6. Example of FM-CW system output (Joe Wright SNOTEL site, 5-2-81).

liquid water content determinations were combined in a weighted average, based on the thickness of uniform wetness layers, to provide a liquid water content value representative of the entire profile.

3.2 Model Comparison with Raw Data

The ground truth and microwave data collected in this study is presented in Table 1. The very limited nature of this data set relegates it to a position quite short of conclusive confirmation, but it does offer some encouragement. Table 1 shows the ground-truth/model-predicted values of the relative dielectric constant ε'_{sp}, and the FM-CW measured values ε'_{sm}. Also included in this table are values from Sweeny and Colbeck, 1974, the only other relevant data available in raw form. Sweeny and Colbeck measured the dielectric constant of snow samples emplaced in a slotted wave guide using microwaves at 6 GHz. An elaborate ice-bath jacket surrounded the sample cell, and great pains were taken to maintain a liquid-water mass balance as they added known quantities of 0^{o} C water to 0^{o} C snow in a controlled temperature environment.

In making these model/data comparisons, it is useful to note that the porosity $\phi = \theta_a + \theta$, where θ_a and θ are the volumetric contents of air and water respectively, and[1] $\rho_s = (1 - \phi)\,\rho_i + \theta\rho_w$, where $\rho_i = 0.917$ g/cm^3. The depths of these components (d_a, d_w, d_i) are set numerically equal to their respective volumetric contents; i.e., $d_a = \theta_a$, $d_w = \theta$, and $d_i = (1 - \phi)$, assuming a unit snow depth.

---

[1] See list of symbols for definition of terms

In Table 1, the squared error of the ground-truth/model-predicted dielectric constant vs the measured dilectric constant gives both a feeling for how well the dielectric mixture model performs and an idea of the degree of scatter in the data. Note the high degree of scatter (mean squared error = 0.3036) in Sweeny and Colbeck's data. Despite their special precautions, they attribute this scatter to the lack of calorimeter measurements to confirm liquid water contents (Colbeck, 1980). The relative error of predicted vs measured dielectric constant gives a better idea of the model performance, because the sign of the error (negative or positive) is retained, thus tending to eliminate the effects of scatter when an average is taken. As shown in Table 1, the mean relative error associated with the FM-CW data is 0.0134 and the mean relative error associated with Sweeny and Colbeck's data is -0.0113. Although it is dangerous to draw any conclusions from such a small data set, it appears that the model-predicted values fall slightly high compared to the FM-CW measurements and slightly low compared to Sweeny and Colbeck's measurements.

It should be noted that regardless of the large amount of scatter in Sweeny and Colbeck's data, the imaginary part of the complex dielectric constant of wet snow which they measured[2] (shown in Table 1) is very useful in determining the validity of assuming wet snow to be a good dielectric. This is the main assumption which the electrical path length dielectric mixture model for wet snow is predicated upon.

---

[2]The values included in Table 1 do not include the very high water content samples they measured which have large loss tangents. See Sweeny and Colbeck, 1974 for the full data set.

3.3 Model Comparison with Other Models and Data Sets

Table 2 (Stiles and Ulaby, 1981) shows the other dielectric mixture models that have been applied to snow[1]. Some are only applicable to dry snow, as indicated, and all of them have calibration parameters which are adjusted to achieve a "best fit" to the paucity of existing data. All of these formulas try to account for the geometry of the constituent inclusions and their orientation with respect to the polarization of an impressed electrical field. One should bear in mind that these formulas were originally devised to explain capacitance measurements made in condenser cells where a near-perfectly polarized electric field exists across a medium. In addition, the electric fields were either static or low frequency. What is more desirable, for the particular problem at hand, is a model devised to account for the propagation of electromagnetic waves; this is what the electrical path length model attempts to do.

The model of Polder and Van Santen, 1946, is one of the more flexible and well accepted mixture models available. It has been applied in two different ways by Colbeck, 1980, and Ambach and Denoth, 1980, and is shown as formulas 6 and 7 in Table 2. Notice that both of these equations are implicit in ε_{ws} ($\varepsilon_{ws} = \varepsilon_s'$ in this paper) and are distinctly more complicated than the electrical path length model. Also, notice the calibration parameters, A_{ij} and A_{wj} (polarization factors[1]), which are indexed for summation over the three principal axes of the ice and water inclusions. A given shape of these inclusions must be assumed in order

---

[1] See list of symbols for definition of terms.

TABLE 2

Mixing Formulas for Snow

Formula Number	Mixing Formula [1]	Comments	Inclusion Shape	Reference
1	$\frac{\epsilon_{ds} - 1}{3\epsilon_{ds}} = V_i \frac{\epsilon_i - 1}{\epsilon_i + 2\epsilon_{ds}}$	Simplification or 6 for spherical with $V_w = 0$ $\epsilon_{ws} = \epsilon_{ds}$	Spherical	Cumming, '52 Glen and Paren
2	$\frac{\epsilon_{ds} - 1}{\epsilon_{ds} + F} = V_i \frac{\epsilon_i - 1}{\epsilon_i + F}$	Dry snow only	F = 0 vertical to F = ∞ planar	Evans (Weiner for dry snow)
3	$\epsilon_{ws} = \frac{\epsilon_w V_w U + \epsilon_{ds}(1-V_w)}{V_w U + (1-V_w)}$ where $U = \frac{\epsilon_{ds} + F}{\epsilon_w + F}$	Wet snow	F = 0 vertical to F = ∞ planar	Edgerton et.al. (Weiner)
4	$\epsilon_{ds}^{1/3} - 1 = V_i(\epsilon_i^{1/3} - 1)$	Dry snow	Spherical	Glen and Paren (Looyenga)
5	$\epsilon_{ws} - \epsilon_{ds} = \frac{V_w}{3}(\epsilon_w - \epsilon_{ds}) \sum_{j=1}^{3} \frac{1}{1 + (\frac{\epsilon_w}{\epsilon_n} - 1)A_{wj}}$	ϵ_n - local dielectric constant accounts for particle interactions	Ellipsoidal	Sweeney and Colbeck, '74 (de Loor)
6	$\epsilon_{ws} = 1 + \frac{\epsilon_{ws}}{3} V_i(\epsilon_i - 1) \sum_{j=1}^{3} \frac{1}{\epsilon_{ws} + (\epsilon_i - \epsilon_{ws})A_{ij}} + \frac{\epsilon_{ws}}{3} V_w(\epsilon_w - 1) \sum_{j=1}^{3} \frac{1}{\epsilon_{ws} + (\epsilon_w - \epsilon_{ws})A_{wj}}$	Different shape factors for water and ice	Ellipsoidal	Colbeck, '80 (Polder and van Santen)
7	$\epsilon_{ws} - \epsilon_{ds} = \frac{V_w}{3}(\epsilon_w - \epsilon_{ds})\epsilon_{ws} \sum_{j=1}^{3} \frac{1}{\epsilon_{ws} + (\epsilon_w - \epsilon_{ws})A_{wj}}$	Simplification of 5 with $\epsilon_n = \epsilon_{ws}$	Ellipsoidal	Ambach and Denoth, '80 (Polder and van Santen)
8	$\epsilon_{ds} = 1 + \frac{3V_i(\epsilon_i - 1)}{(2 + \epsilon_i) - V_i(\epsilon_i - 1)}$	Simplification of 9	Spherical	Tinga et.al. '73
9	$\epsilon_{ws} = 1 + \left\{ 3 \left[(\frac{r_w}{r_a})^3 (\epsilon_w - 1)(2\epsilon_w - \epsilon_i) - (\frac{r_i}{r_a})^3 (\epsilon_w - \epsilon_i)(2\epsilon_w + 1) \right] \right.$ $\times \left[(2 + \epsilon_w)(2\epsilon_w + \epsilon_i) - 2(\frac{r_i}{r_w})^3 (\epsilon_w - 1)(\epsilon_w - \epsilon_i) \right.$ $\left. \left. - (\frac{r_w}{r_a})^3 (\epsilon_w - 1)(2\epsilon_w + \epsilon_i) + (\frac{r_i}{r_a})^3 (\epsilon_w - \epsilon_i)(2\epsilon_w + 1) \right]^{-1} \right\}$		Spherical of ice coated with water	Tiuri and Schultz, '80 (Tinga et.al.)

[1] See list of symbols for definition of terms.

to use this model. Figure 7a compares theoretical curves generated by the electrical path length model and the Polder and Van Santen model (as applied by Cumming, 1952) for the dry snow case. Spherical ice grains were assumed in the application of Polder and Van Santen's model in this figure, and the electrical path length model agrees well. Cumming measured the snow dielectric constant or permittivity using a wave guide technique similar to Sweeny and Colbeck, except at a frequency of 9.37 GHz.

Figures 7b and 7c compare the electrical path length model to Ambach and Denoth's data, along with three other models. The Wiener and Looyenga models are shown on Table 2 as formulas 2 and 4 respectively. In the 1972 paper from which this figure is taken, Ambach and Denoth felt that the Wiener model was superior. They have since become believers in Polder and Van Santen's model (Ambach and Denoth, 1980), which compares very closely to the electrical path length model. Ambach and Denoth measured the dielectric constant in a capacitance cell operating at 20 MHz.

It should be pointed out that the prediction of dry snow dielectric constant is a relatively simple task because it is a function of snow density only; the Looyenga model yields the simple form

$$\varepsilon_s' = (1 + 0.508\rho_s)^3 \qquad (21)$$

However, when liquid water is present in the snow mixture, the dielectric constant becomes a function of water content and operating frequency, as well as snow density (this is why many workers prefer the ther permittivity over the misleading term, dielectric "constant"). Thus in the

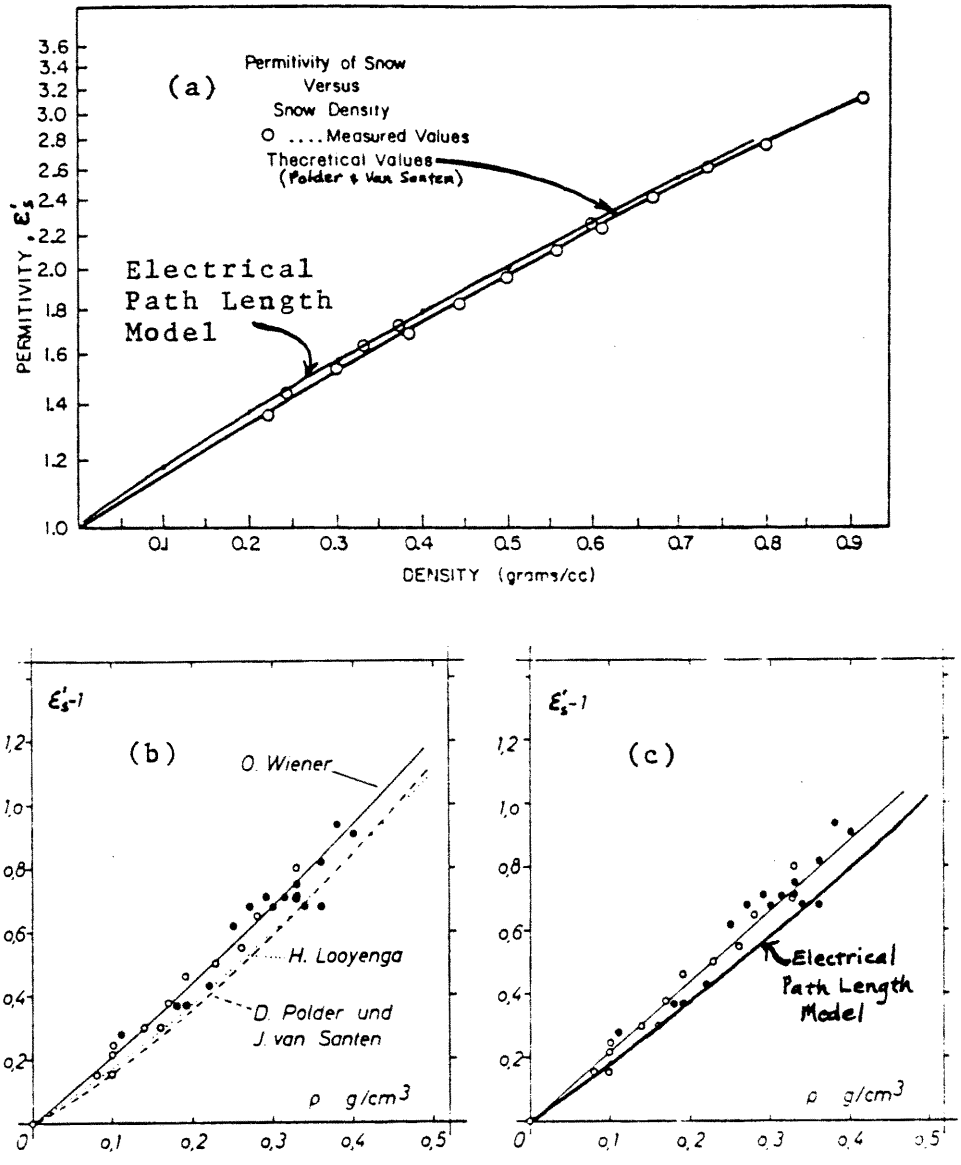

Figure 7. Model/data comparisons for the dry snow case.

a) Data from Cumming, 1952, shown with a curve predicted by the Polder and Van Santen model and the electrical path length model curve.

b) Ambach and Denoth's data for $\varepsilon'_s - 1$ vs snow density. Empty circles stand for fine-grained and full circles stand for coarse-grained snow samples. Three dielectric mixture model curves are shown along with this data.

c) A regression line through Ambach and Denoth's data is compared to the electrical path length model curve. Note that no systematic difference exists between the coarse-grained and fine-grained snow samples (Ambach and Denoth, 1972).

figures to be discussed presently, for the wet snow case, two of the three independent variables must be specified as constants in order to display two-dimensional graphs.

Figure 8a shows the electrical path length model in comparison with Ambach and Denoth's data and a regression line. Cold calorimetry was employed for the liquid water determinations, and the electrical path length model fits the data very well. Figure 8b is included to emphasize the empirical nature of the Wiener model, which includes a formzahlen factor which can be adjusted to fit a wide variety of data. It should be noted that due to the natural variability of snow, the samples measured will vary in density, so that this independent variable cannot be held truely constant. In order to plot such data on a two-dimensional graph, attempts are made to remove the effects of density on the dielectric constant, as shown on Figure 8. This is also done in the plots of Sweeny and Colbeck's data (partial list in Table 1) on Figure 11, discussed later. It appears that this practice of "density reducing" the data is only partially effective, but it is the only way to display two-dimensional graphs.

Figure 9 shows a comparison to Linlor's data (Linlor, et. al., 1980). Notice that unlike the other worker's graphs, Linlor plots the dielectric constant as a function of frequency while holding the liquid water content constant. His instrumentation is the only in use that records system response over a wide range of frequency. He employed a sweep-frequency radar with one-way propagation through an open Plexiglas sample box similar to the one used in the present study, although his box measured only 39 cm by 39 cm in the plane perpendicular to the microwave

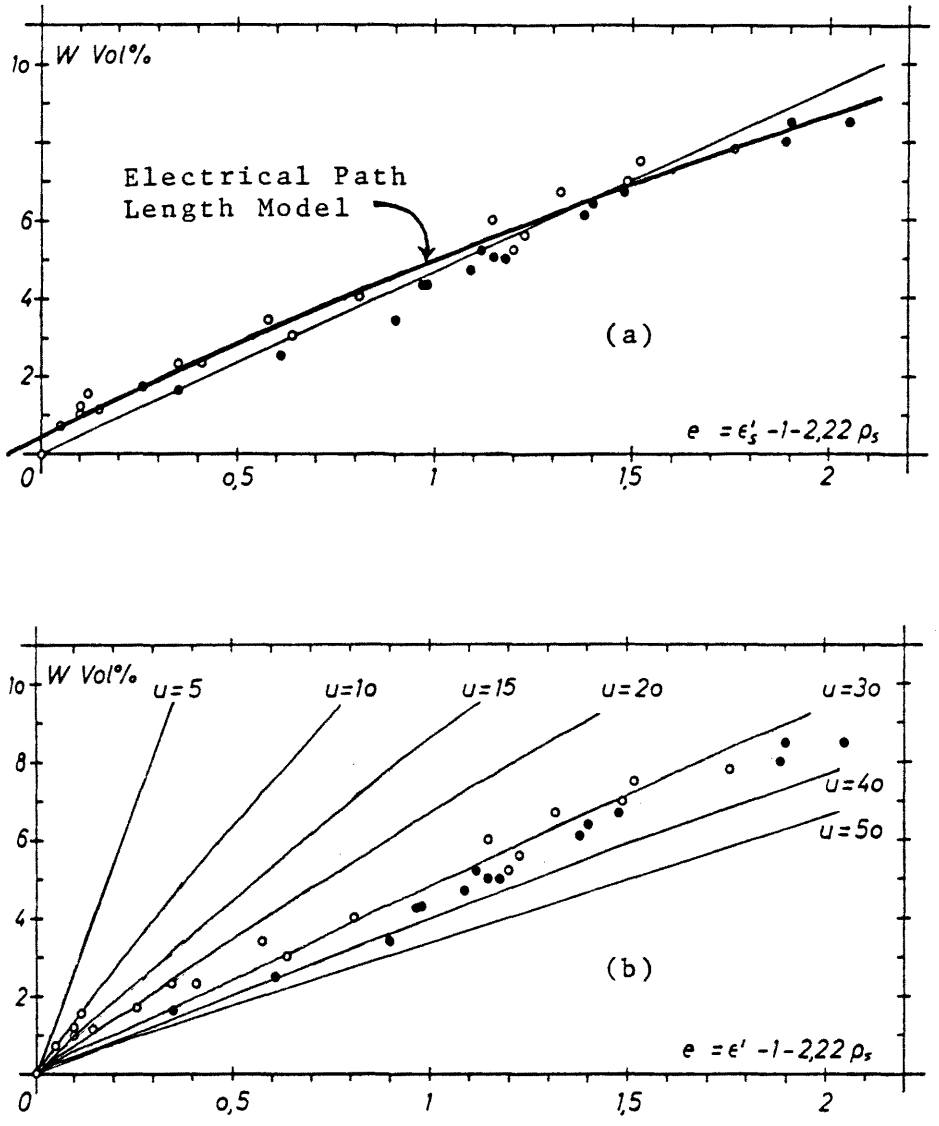

Figure 8. Model/data comparison for wet snow.

a) Data points of Ambach and Denoth, 1972, with a regression line through the data. Also shown is a theoretical curve generated from the electrical path length model with $\rho_s = 0.32$ g/cm^3 and $\varepsilon'_w = 87.91$ and f = 20MHz.

b) The family of curves generated by Wiener's model (formula 3, table 2) for different values of the formzahlen factor "u".

Note: plotting ($e = \varepsilon'_s - 1 - 2.22\rho_s$) is an attempt to "density reduce" the data.

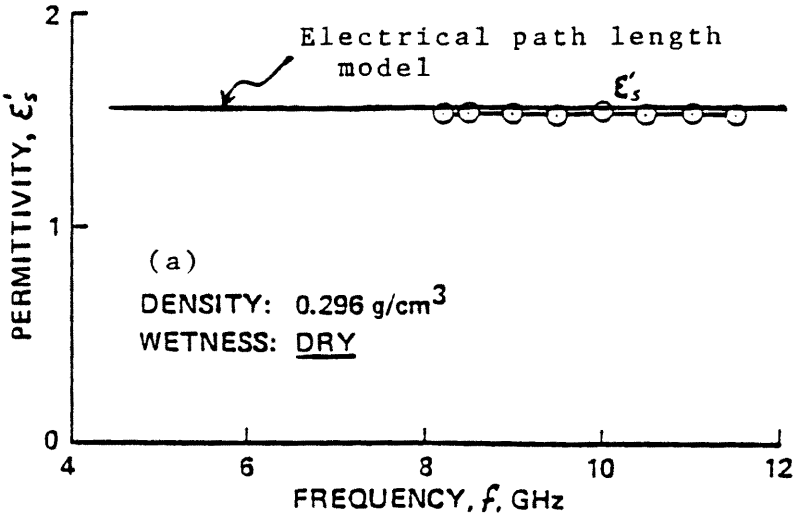

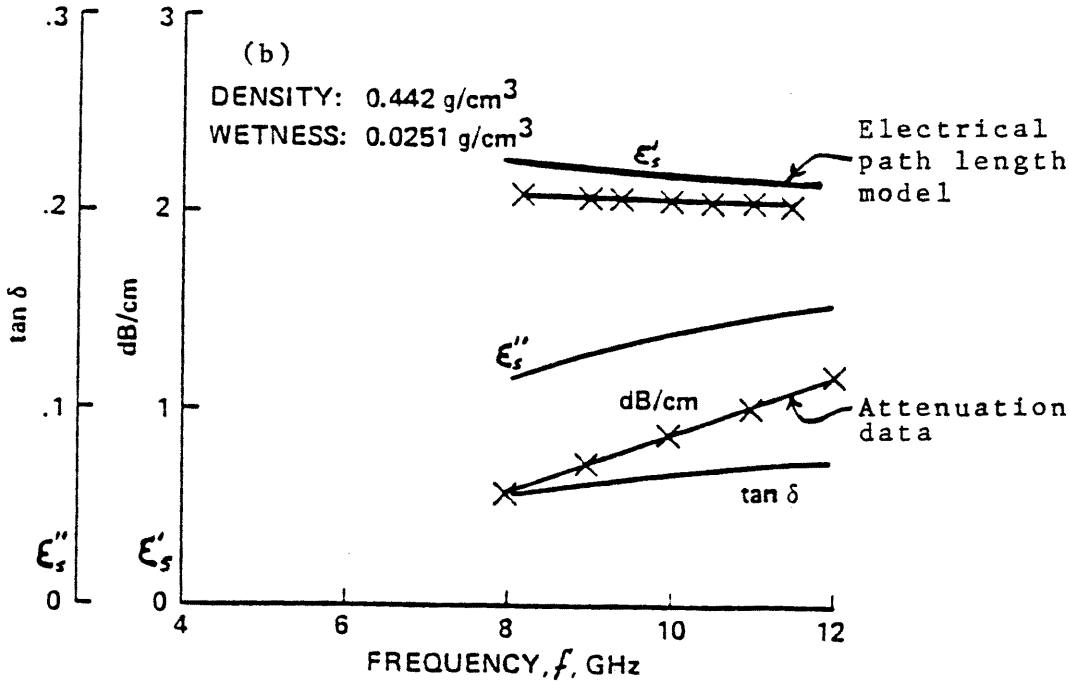

Figure 9. Model comparison to the data of Linlor, et.al.,1980.

a) Linlor's data on the dielectric constant of dry snow, shown with the electrical path length model curve.

b) Linlor's data on the real and imaginary parts of the dielectric constant, attenuation, and the loss tangent (tan δ) for wet snow, shown with the corresponding curve for the electrical path length model.

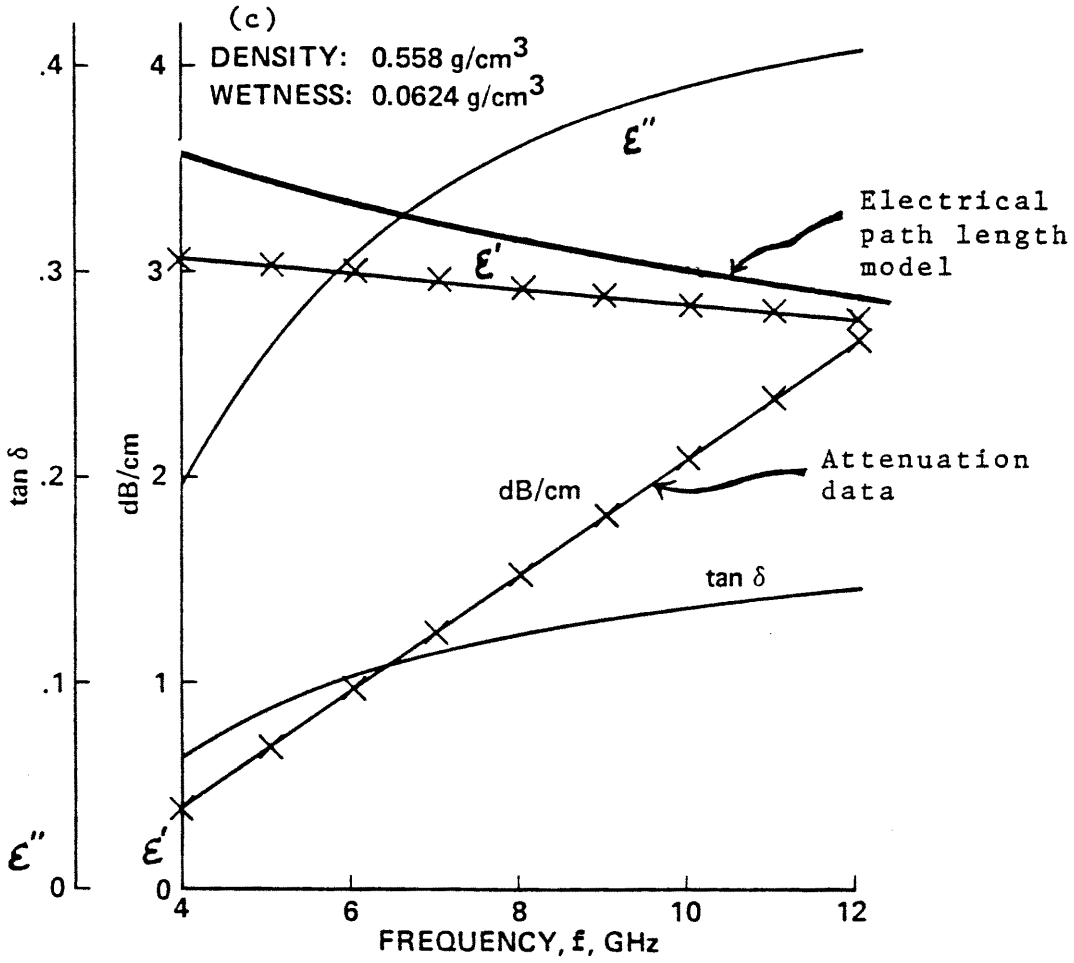

Figure 9c. Linlor's data on the real and imaginary parts of the dielectric constant, attenuation, and the loss tangent (tan δ) for wet snow, shown with the corresponding curve for the electrical path length model.

beam. Linlor also attempted a mass balance approach for liquid water determinations instead of the preferred cold calorimetry. The dry snow values shown in Figure 9a agree very well with the electrical path length model, as should be expected. The model comparisons with the wet snow data presented in Figures 9b and 9c are not as close, but reasonable. The electrical path length curves fall a bit high compared to the measured values in this case. It should be noted that the values reported on these figures for the imaginary part of the dielectric constant ε_s'' indicate that the loss tangent ($\varepsilon''/\varepsilon'$) for wet snow would be small enough to neglect under the frequency and wetness restrictions given previously (good dielectric assumption made in order to arrive at equation 14). The imaginary part of the dielectric constant is obtained experimentally by measuring the phase shift (degrees) and attenuation (dB/cm) of radiation as it propagates through the dielectric medium (see Linlor, et.al., 1980; Sweeny and Colbeck, 1974).

It should be pointed out that although this present study utilized only the velocity of propagation (and thus only the real part of the dielectric constant) in measuring snowpack properties, a great potential exists in systems that could also utilize attenuation information.

Figure 10 shows the electrical path length model compared to the data of Tobarias, et. al., 1978. Nothing is known of Tobarias' data other than the curves presented here. The electrical path length model predicts only the real part of the complex dielectric constant ε_s', so there is no curve for it shown on the graph of the imaginary part. This graph is included here to provide further evidence that wet snow can be considered to be a good dielectric (with frequency

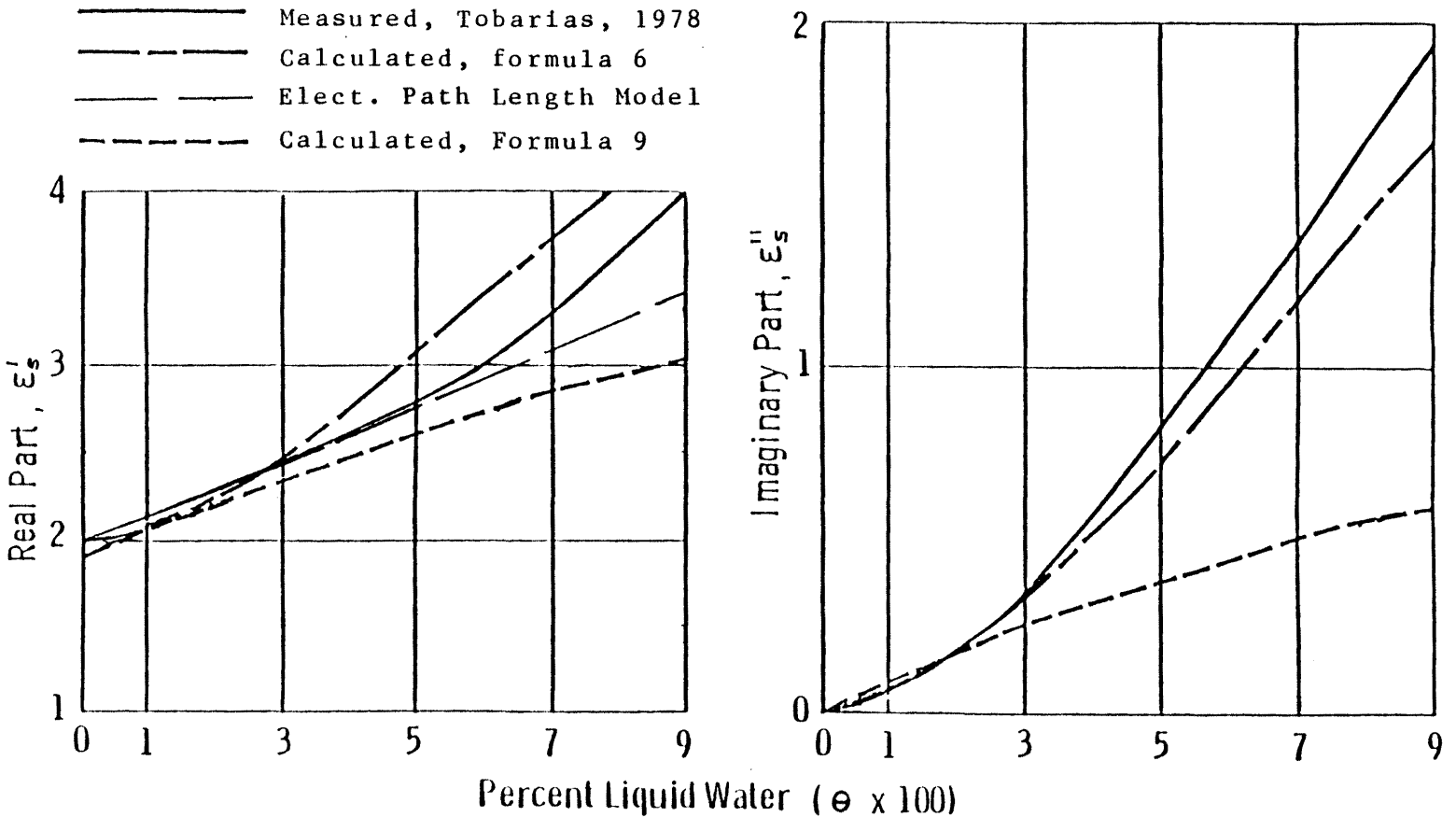

Figure 10. Real and imaginary parts of the relative dielectric constant of snow as a function of liquid water content at f = 9.4 GHz, with ρ_s = 0.5 g/cm^3 and ε_w'(f = 9.4 GHz) = 42.29. (from Stiles and Ulaby, 1981).

Note: The electrical path length model curve is coincident with Tobarias' data curve up to a liquid water content of 5% by volume.

and wetness restrictions). Note that the observation frequency used in Tobarias' data collection was 9.4 GHz; at this frequency, the relative dielectric constant of liquid water equals 42.29, as shown in the figure. Because this frequency exceeds the imposed limit of 6 GHz, the wet snow appears to become significantly lossy at water contents greater than 5% by volume. It may be more than just coincidence that the electrical path length model curve matches the data curve exactly up to a liquid water content on 5% by volume.

Figure 11 shows the electrical path length model compared to Sweeny and Colbeck's data (including the very high water content values). It appears that the model predicts somewhat low when compared to this data set, however, at water contents below 8% by volume, the discrepancy is not statistically significant, given the degree of scatter in the data. Notice how poorly the model of Tinga, et. al., 1973, as applied by Tiuri and Schultz, 1980 (formula 9 of Table 2) fits the data at high water contents. This is due to the incorrect assumption that the snow mixture consists of spherical ice grains coated with uniform layers of liquid water. This is an impossible configuration, because the grains are in contact with each other and the liquid water inclusions reside as fillets and veins between the grains (Colbeck, 1980).

Figure 12 is included to further emphasize the empirical nature of these currently accepted mixture models. The Polder and Van Santen model, as applied by Colbeck, 1980, uses an "aspect ratio" to describe the shape of liquid water inclusions. This "n" value can be varied to adjust the model to fit a wide variety of data. Colbeck found that an aspect ratio of n = 3.5 made for the best fit to the data of Ambach and

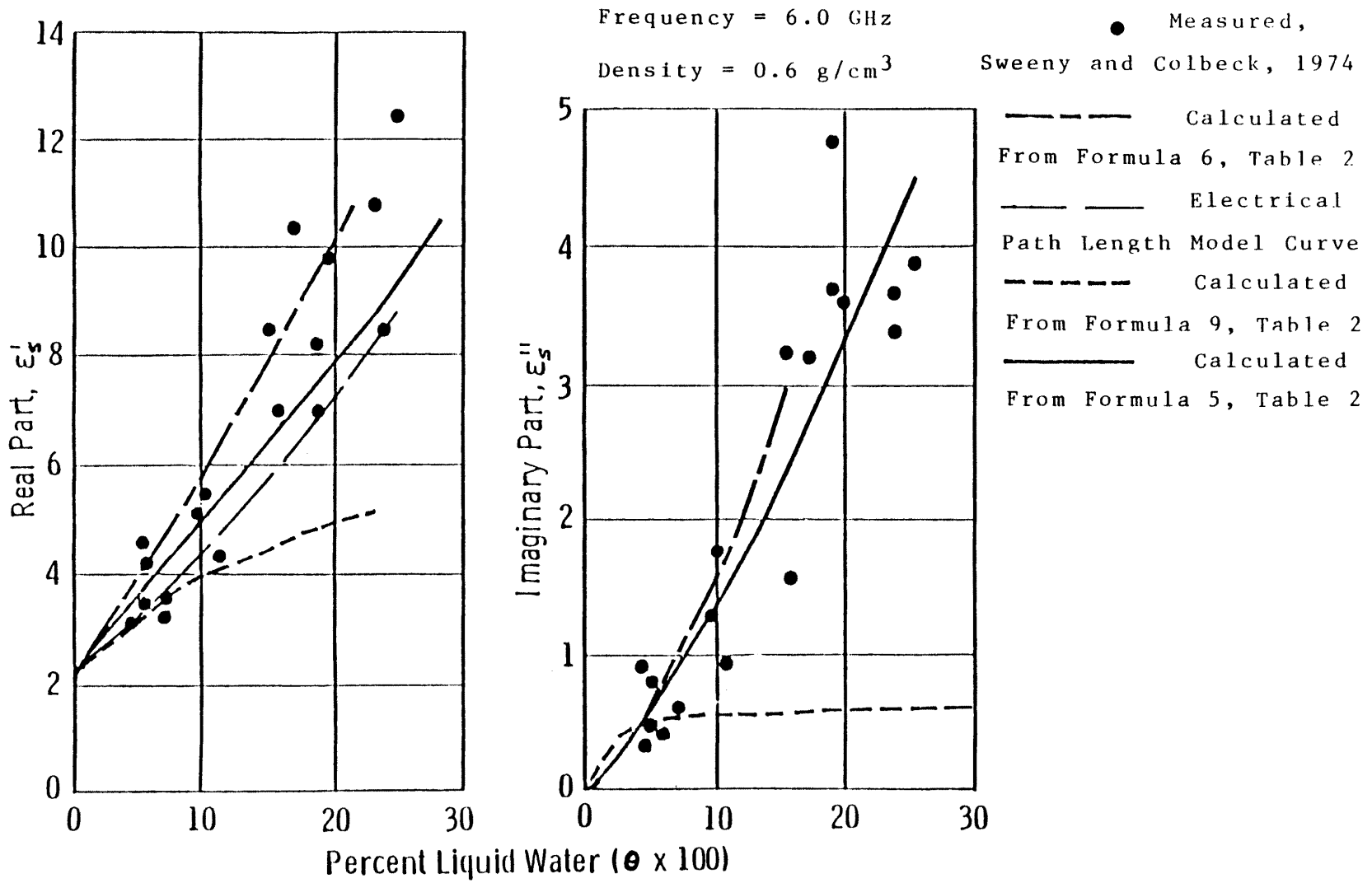

Figure 11. Real and imaginary parts of the dielectric constant of snow as a function of liquid water content at 6 GHz, $\varepsilon'_w = 60.35$ (modified from Stiles and Ulaby,81).

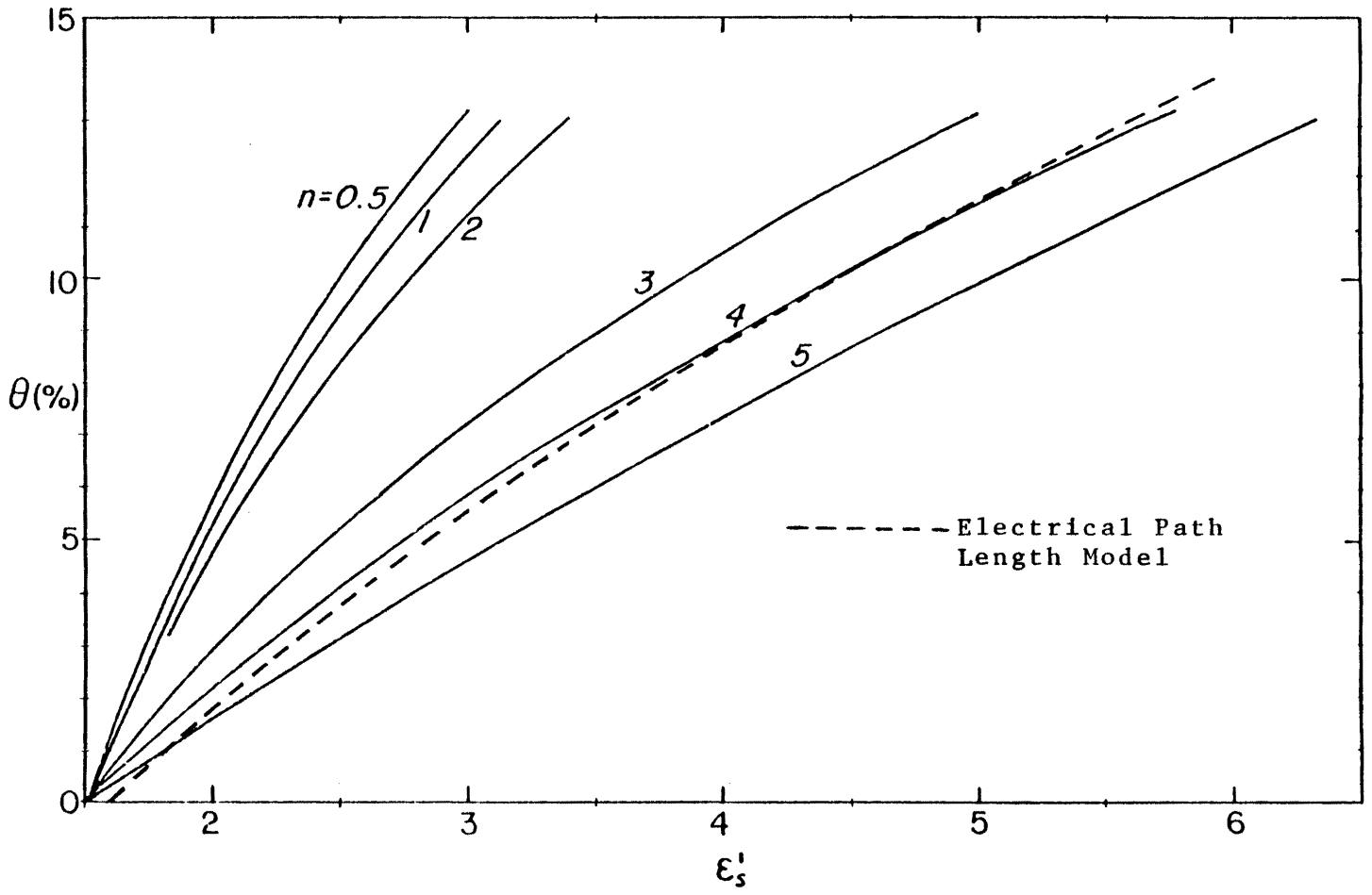

Figure 12. Calculated values of the dielectric constant (from formula 6, table 2) vs liquid water content for various values of the aspect ratio "n". Porosity = 0.651. Colbeck, 1980 found that an aspect ratio of 3.5 made for a good fit to his data. Also shown is a curve generated from the electrical path length model, with $\varepsilon'_w = 87.91$.

Denoth, 1972, and Sweeny and Colbeck, 1974. The electrical path length model curve is plotted against these curves, and falls near the n = 4 curve.

To summarize, suffice it to note that the electrical path length model curves fall above some data sets and model curves, and below others. In most cases the agreement is quite close, especially at water contents less than 8.0% by volume.

Reasons for preferring the electrical path length model include:

1. its simplicity; it is easy to work with,
2. it is especially designed for use with active microwave systems, and
3. it is physically based, with no empirical parameters needing calibration.

CHAPTER IV

SOLVING FOR THE WATER EQUIVALENCE OF A WET SNOWPACK

Up to this point, we have appeared more interested in finding the dielectric constant of the snow as a function of its constituent properties than in finding the snow's hydrologic properties as a function of the measured dielectric constant. It should be realized that this is simply a model verification procedure, and it is still our aim to be able to remotely sense snow properties with no prior ground truth knowledge.

To this aim, equation (20) is re-examined. The FM-CW measures the dielectric constant of the snow ε_s' with the aid of equation (17), where the depth of snow d_s must be known. Note that in the avalanche path configuration (Figure 4), there is no immediately obvious way to measure the snowpack depth, especially considering the large stresses downslope snow creep would create on any structure penetrating the snowpack. Thus, only semi-quantitative determinations of loading rates, water equivalence, and liquid water content could be made in this particular application. The accuracy of water equivalence and loading rate determinations would depend on how accurately the snow density could be estimated in the case of dry snow, and there exist methods for such estimation. If the snow had liquid water present, the accuracy of all determinations would hinge on diurnal measurements in which a complete draining and/or freezing of the liquid water could be assured for night-time measurements.

In the hydrometeorologic data acquisition configuration (Figure 3), the distance from the FM-CW to the soil is a known fixed distance, and the range detection capabilities of the radar can be used to measure d_{fs} and thus d_s. Once the depth of snow is known, equation (20) appears as one equation with two unknowns, the depth of ice d_i and the depth of water d_w. If the snowpack is dry ($d_w = 0$), our problem is already solved, but for the wet snow case another equation is needed. This equation comes from the fact that $\varepsilon'_w = \varepsilon'_w(f)$ and $\varepsilon'_s = \varepsilon'_s(f)$ in the microwave region, whereas ε'_i = constant. Thus, subscripting the dielectric constants in equation (19) with appropriate measurement frequencies, we get two equations with two unknowns

$$\sqrt{\varepsilon'_{s2}}d_s = \sqrt{\varepsilon'_{w2}}d_w + \left[d_a + \sqrt{\varepsilon'_i}d_i \right] \tag{22}$$

and

$$\sqrt{\varepsilon'_{s5}}d_s = \sqrt{\varepsilon'_{w5}}d_w + \left[d_a + \sqrt{\varepsilon'_i}d_i \right] \tag{23}$$

The quantity in brackets above would be a constant, and we can solve for d_w, the depth of water

$$d_w = \frac{d_s\left(\sqrt{\varepsilon'_{s2}} - \sqrt{\varepsilon'_{s5}}\right)}{\left(\sqrt{\varepsilon'_{w2}} - \sqrt{\varepsilon'_{w5}}\right)} \tag{24}$$

The numerator of equation (24) consists of values that would be measured by an active microwave system, whereas the denominator is a known constant. Once determined, the value of d_w from equation (24) can be plugged into equation (20), slightly rearranged

$$\sqrt{\varepsilon'_s}d_s = 0.775d_i + d_s - d_w + \sqrt{\varepsilon'_w}d_w \tag{20b}$$

where the only unknown would then be d_i, the depth of ice.

Solving for d_i gives

$$d_i = \frac{d_s(\sqrt{\varepsilon'_s} - 1) + d_w(1 - \sqrt{\varepsilon'_w})}{0.775} \tag{25}$$

The water equivalence is given by

$$WE = 0.917 d_i + d_w \tag{26}$$

and the liquid water content is

$$\theta = \frac{d_w}{d_s} = \frac{d_w}{d_i + d_a + d_w} \tag{27}$$

The accuracy with which these last two quantities could be measured has not been determined quantitatively. However, the general accuracy levels obtained by Boyne and Ellerbruch, 1979, for dry snow (±5%) should be obtainable in the wet snow case as well (see also Boyne and Ellerbruch, 1980).

Future research activities is this area should direct attention to collecting such dual-frequency data and comparing the results to the water equivalence determined by density profiles or Mount Rose snowtube samples. An experiment could be carried out in this manner without the reliance on cold calorimetry, thus eliminating the arduous task of characterizing a snowpack's liquid water content profile. This was the original intention of this investigator until one of the available FM-CW's broke down. This FM-CW would probably not have been suitable for observing wet snow in any case due to the high frequency of the sweep band (8-12.4 GHz), which is in the range where wet snow becomes a lossy dielectric.

CHAPTER V

OPERATIONAL DESIGN CONFIGURATIONS

Many of the design considerations have already been mentioned, and the basic configurations are depicted in Figures 3 and 4. The metal grate should be placed on level ground with adequate drainage, a known distance from the radar antennas. The grate would allow water to percolate through, but at the same time it would appear opaque to the radar, giving a strong return signal. The instrument tower would, of course, have to be installed in such a manner as to have a negligible effect on local snow deposition patterns.

If an FM-CW is used, it must be capable of sweeping over two different frequency ranges. Recommended ranges are 1-4 GHz and 4-7 GHz, so that the centers of the sweep widths would be at 2.5 and 5.5 GHz respectively. If the frequency was swept over too large a range, there is the possibility that the return signal, after propagating through very wet snow, would not retain its linear form (as shown in Figure 2). This could cause a blurring effect on the system output due to the difference frequencies being averaged over time in the spectrum analyzer. Although no highly wet snow was observed in this study, no problems were encountered in this regard.

A dual-frequency pulse radar could also be used in this application, provided its range resolution was adequate. Pulse radars have the advantage that they emit pulses in a narrow frequency band (1 GHz for a

10^{-9} second pulse width), and thus would not be subject to as much dispersion (blurring), as mentioned above. Taking the propagation velocity in the snowpack to be $v = c/\sqrt{\varepsilon'_s}$, as given by equation (16), the two way propagation time from the radar to the snow/soil discontinuity will be

$$t = 2\left[\frac{d_s\sqrt{\varepsilon'_s}}{c} + \frac{d_{fs}}{c}\right] \tag{28}$$

Solving for the square root of the dielectric constant of the snow gives

$$\sqrt{\varepsilon'_s} = \frac{c}{d_s}\left[\frac{t}{2} - \frac{d_{fs}}{c}\right] \tag{29}$$

which could be determined at two different frequencies to provide the information on water equivalence and liquid water content, given by equations (24) through (27). Recommended operating frequencies for a dual-frequency system are 2 GHz and 5 GHz.

Regardless of whether an FM-CW or pulse radar is used, the system would have to be enclosed in thin plastic if mounted above ground as indicated in Figure 3. Microwaves will penetrate the plastic readily, and with the aid of an internal heat source, this covering would ensure no riming or damage to the equipment by weather. Alternately, the whole configuration in Figure 3 could be inverted, placing the radar in the ground, as in Figure 4. The use of the metal grate as a reflector could then be replaced by a small corner cube (radar reflector) suspended from the tower. This would reduce changes in snow deposition patterns likely to be caused by the presence of a metal plate.

CHAPTER VI

CONCLUSIONS

The simple electrical path length dielectric mixture model seems to adequately describe the response of the FM-CW to a wet snowpack. The model also agrees well with the existing data and the most accepted (though more complicated) dielectric mixture models. With the use of the electrical path length model and dual-frequency microwave data, snowpack water equivalence and liquid water content should be obtainable remotely. In the avalanche forecasting mode, this scheme would yield only qualitative measures of water equivalence, loading rates, and liquid water content. In the hydrometeorological data acquisition platform mode, quantitative determinations could be obtained because the snow depth would be a known quantity. Overall, the measurement system shows great potential for use as an operational remote sensing tool. However, this paper must be concluded on the familiar note that more research is still needed to better determine the accuracy and reliability of the system.

REFERENCES

Ambach, W. and A. Denoth, "Studies on the Dielectric Properties of Snow", Zeitschrift fur Gletscherkunde and Glazialgeologie, Vol. VIII, No. 1-2, 1972, pp. 113-123.

Ambach, W. and A. Denoth, "The Dielectric Behavior of Snow: A Study Versus Liquid Water Content", Proceedings of NASA Workshop on Microwave Remote Sensing of Snowpack Properties, Ft. Collins, Colorado, May, 1980, NASA CP-2135, 1980.

American Society of Photogrammetry, "Manual of Remote Sensing", Vol. I, Falls Church, VA., 1975.

Boyne, H.S. and D.A. Ellerbruch, "Microwave Measurement of Snow Stratigraphy and Water Equivalence", Proceedings of the 47th Annual Western Snow Conference, Sparks, Nevada, April, 1979, pp. 20-26.

Boyne, H.S. and D.A. Ellerbruch, "Active Microwave Water Equivalence Measurements", Proceedings of NASA Workshop on Microwave Remote Sensing of Snowpack Properties, Ft. Collins, Colorado, May, 1980, NASA CP-2153, 1980.

Colbeck, S.C., "Liwuid Distribution and the Dielectric Constant of Wet Snow", Proceedings of NASA Workshop on Microwave Remote Sensing of Snowpack Properties, Ft. Collins, Colorado, May, 1980, NASA CP-2153, 1980.

Cumming, W.A., "The Dielectric Properties of Ice and Snow at 3.2 Centimeters", Jour. Appl. Physics, Vol. 23, No. 7, 1952, pp. 768-773.

Ellerbruch, D.A. and D.R. Belsher, "Electromagnetic Technique of Measuring Coal Layer Thickness", IEEE Transactions on Geoscience Electronics, Vol. GE-16, No. 2, 1978, pp. 126-133.

Ellerbruch, D.A. and H.S. Boyne, "Snow Stratigraphy and Water Equivalence Measured with an Active Microwave System", Jour. of Glaciol., Vol. 26, No. 94, 1980, pp. 225-233.

Fletcher, N.H., "The Chemical Physics of Ice", Cambridge University Press, 1970.

Goodison, B.E., et. al., "Measurement and Data Analysis", Handbook of Snow: Principles, Processes, Management, and Use, D.M. Gray and D.H. Male, editors, Pergamon Press, 1981.

Hasted, J.B., "Aqueous Dielectrics", Chapman and Hall, London, 1973.

Johnk, C.T.A., "Engineering Electromagnetic Fields and Waves", John Wiley and Sons, Inc., New York, 1975.

Jones, E.B., et. al., "Measurement of Liquid Water Content in a Melting Snowpack Using Cold Calorimeter Techniques", Proceedings of NASA Workshop on Microwave Remote Sensing of Snowpack Properties, Ft. Collins, Colorado, May, 1980, NASA CP-2135, 1980.

Linlor, W.I., et. al., "Snow Electromagnetic Measurements", Proceedings of NASA Workshop on Microwave Remote Sensing of Snowpack Properties, Ft. Collins, Colorado, May, 1980, NASA CP-2135, 1980.

Looyenga, H., "Dielectric Constants of Heterogeneous Mixtures", Physica 31, 1965, pp. 401-406.

Perla, R.I. and M. Martinelli, Jr., "Avalanche Handbook", Agricultural Handbook 489, USDA Forest Service, Ft. Collins, Colorado, 1976.

Royer, G.M., "The Dielectric Properties of Ice, Snow, and Water at Microwave Frequencies and the Measurement of the Thickness of Ice and Snow Layers with Radar", Technical Report No. 1242, Communications Research Centre, Ottawa, Canada, 1973.

Polder, D and J.H. Van Santen, "The Effective Permeability of Mixtures of Solids", Physica, Vol. II, No. 5, 1946, pp. 257-271.

Shafer, B.A., "Evolution of Snow Sensors and the Potential of Microwave Devices in Operational Telemetry Networks", Proceedings of NASA Workshop on Microwave Remote Sensing of Snowpack Properties, Ft. Collins, Colorado, May, 1980, NASA CP-2135, 1980.

Smith, F.W. and H.S. Boyne, "Snow Pillow System Bheavior for SNOTEL Application", Final Report for the Period Sept. 1980 through Dec. 1981, Soil Conservation Service, USDA. Cooperative Agreement Number 58-8B05-9-177.

Sommerfeld, R.A. and E. LaChapelle, "The Classification of Snow Metamorphism", Jour. of Glaciol., Vol. 9, No. 55, 1970, pp. 3-17.

Stiles, W.H. and F.T. Ulaby, "Dielectric Properties of Snow", NASA CR 166764, December, 1981.

Sweeny, B.D. and S.C. Colbeck, "Measurements of the Dielectric Properties of Wet Snow Using a Microwave Technique", Res. Report 325, U.S. Army CRREL, Hanover, N.H., 1974.

Tinga, W.R. and W.A.G. Voss, "General Approach to Multiphase Dielectric Mixture Theory", Jour. of Applied Physics, Vol. 44, No. 9, 1973, pp. 3897-3902.

Tiuri, M. and H. Schultz, "Theoretical and Experimental Studies of Microwave Radiation from a Natural Snow Field", Proceedings of NASA Workshop on Microwave Remote Sensing of Snowpack Properties, Ft. Collins, Colorado, May, 1980, NASA CP-2135, 1980.

Tobarias, J., et. al., "Determination of the Water Content of Snow from the Study of Electromagnetic Wave Propagation in the Snow Cover", Jour. of Glaciol., Vol. 20, No. 84, 1978, pp. 585-592.

Vickers, R.S. and G.C. Rose, "High Resolution Measurements of Snowpack Stratigraphy Using a Short Pulse Radar", Proceedings of the 8th Int. Symposium on Remote Sensing of Environment, Univ. of Michigan, Ann Arbor, 1972, Vol. I, 1973, pp. 261-277.

Wiener, O., "Zur Theorie der Refraktion Skonstanten", Berichte Gasellschaft der Wissen Schaften zu Leipzig, Mathematisch-Physikalishe, Bd. 62, Ht. 5, 1910, pp. 256-277.

APPENDIX A

DIELECTRIC RELAXATION PROCESSES

A.1 Polarization Processes

The effect of charge movement within a dielectric medium upon an electric field is called polarization. There are three polarization processes of concern in microwave remote sensing of snowpacks: ionic, electronic, and dipolar. All three result in the development of an opposing electric field within the medium which tends to weaken the impressed electric field locally. The magnitude of this tendency is directly related to the degree of polarization that occurs within the dielectric medium (quantified by the dielectric constant or permittivity, which is a function of the impressed $\overline{E}$ field frequency as well as the medium properties). Electronic, ionic, and dipolar polarization processes operate over different frequency ranges and result in differing degrees of polarization.

Dielectric relaxation is the process responsible for the steep segments of the $\varepsilon_r'(f)$ graph shown in Figure A1. These steep segments depict transitional stages where given polarization processes cease to function due to inertial constraints as frequency increases. This is discussed further in the next section.

Electronic polarization is the response of electron configurations to an impressed electric field. The electron clouds are displaced relative to their nuclei, resulting in a small degree of polarization.

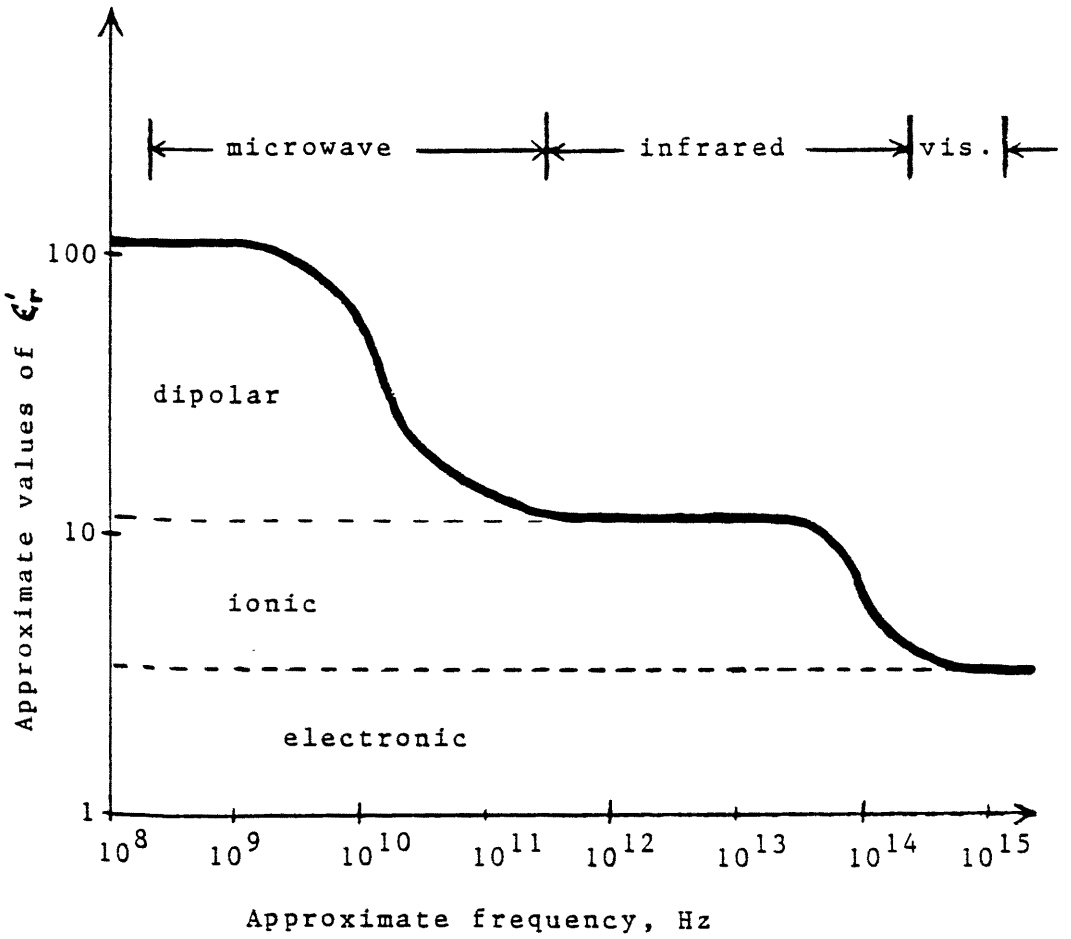

Figure A1. Plot of the relative dielectric constant vs frequency showing the approximate magnitudes associated with various polarization processes and the approximate frequency ranges in which corresponding dielectric relaxations would occur in a hypothetical dielectric medium.

Because the mass of an electron is very small, this polarization process can be effective up to frequencies in the ultraviolet range (10^7 GHz). This process will, of course, function at all other lower frequencies.

Ionic polarization occurs only in crystalline solids, and is a result of displacement of some ions in the lattice relative to others. Because the relaxation time (i.e., the mechanical response time - a function of the inertial mass of protons and neutrons in this case) for this crystal lattice deformation is longer than that for electronic polarization, ionic polarization functions only in response to thermal IR and longer wavelengths. However, the degree of polarization which results is greater, as indicated on Figure A1. It should be noted that the electronic polarization process continues to operate in these lower frequencies, and the total polarization is a result of both processes.

Dipolar polarization results in an even greater degree of polarization and thus a higher dielectric constant for those materials and frequencies in which we see this process (e.g., liquid water at the lower microwave frequencies - see Figure A2). Dipolar polarization is the response of dipolar molecules to an impressed electric field; the dipoles tend to assume an orientation that acts to counter the intensity of that electric field. The inertial constraints on dipolar molecules are relatively great, and therefore this polarization process occurs only up to frequencies of about 10^3 GHz. It is this dipolar polarization process, and the associated dipolar dielectric relaxation process, which is of greatest concern in the microwave remote sensing of snow.

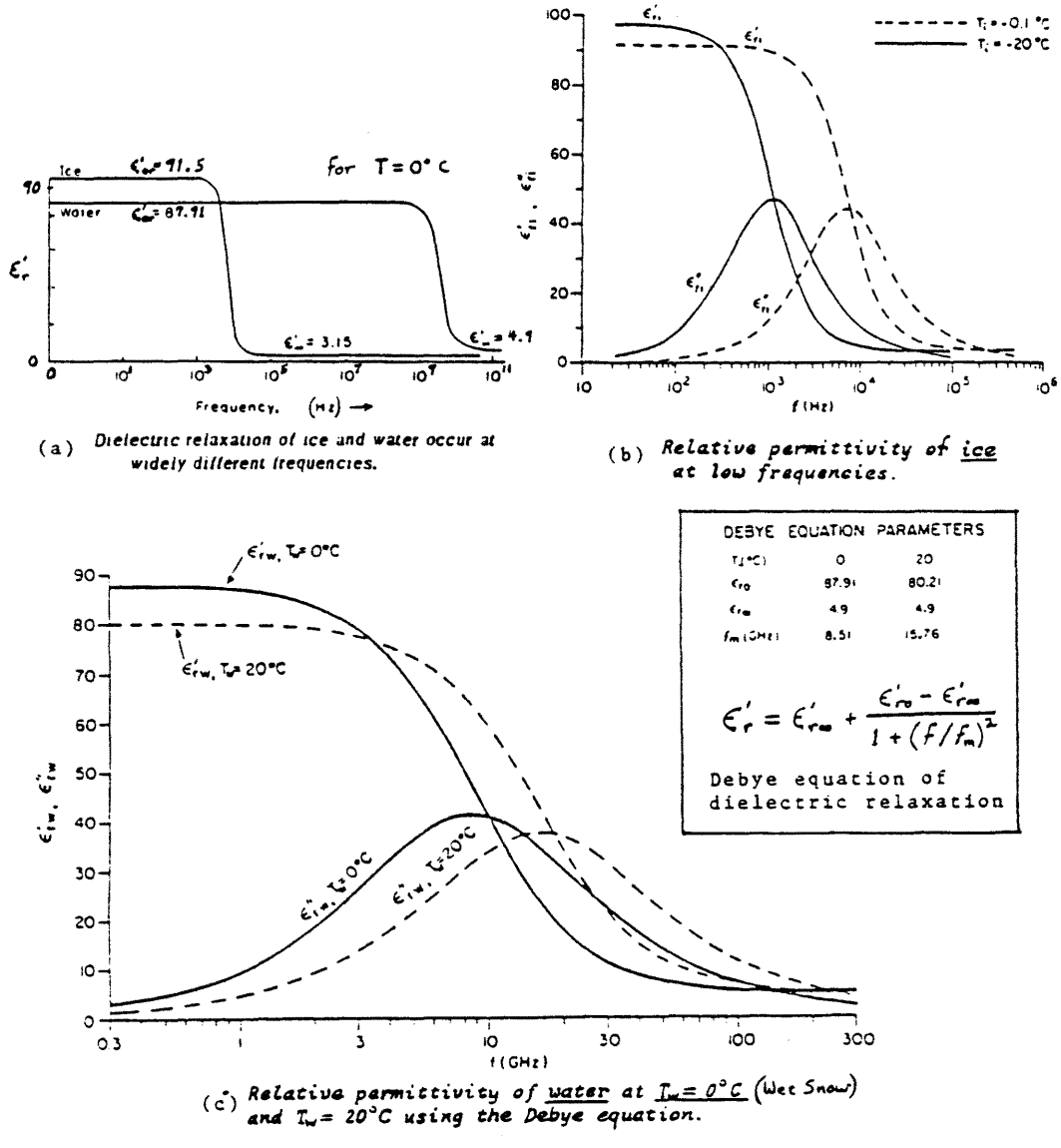

(a) *Dielectric relaxation of ice and water occur at widely different frequencies.*

(b) *Relative permittivity of ice at low frequencies.*

T_i (°C)	0	20
ϵ_{ro}	87.91	80.21
$\epsilon_{r\infty}$	4.9	4.9
f_m (GHz)	8.51	15.76

$$\epsilon_r' = \epsilon_{r\infty}' + \frac{\epsilon_{ro}' - \epsilon_{r\infty}'}{1 + (f/f_m)^2}$$

(c) *Relative permittivity of water at $T_w = 0°C$ (Wet Snow) and $T_w = 20°C$ using the Debye equation.*

Figure A2. Relative dielectric constants of ice and water, showing the associated dielectric relaxations (from Royer, 1973).

A.2 Dipolar Dielectric Relaxation and Losses

The dielectric relaxation process mentioned previously will now be elaborated upon. The displacement flux density $\overline{D}$ will be a sinusiodal function of time, varying from positive to negative, under the influence of a radar-generated electric field $\overline{E}$ which is also a sinusiodal function of time. So long as the frequency with which $\overline{E}$ is varying is not too high (with respect to the ability of the dipoles to undergo necessary polarity reversals), the displacement flux and the electric field remain 90^{o} out of phase. This condition assures a lossless interaction where a maximum dielectric constant is exhibited. However, as frequency is increased, inertial constraints begin to cause a lag in the response of the dipoles. The phase relationship between the displacement flux and the electric field becomes such that energy is dissipated (usually in the form of heat) and the dielectric constant drops due to this inefficiency of the dipoles. It is in this frequency range that the dielectric is termed "lossy".

The frequency at which losses are a maximum is terned the relaxation frequency and is depicted in Figure A2 as inflection points on the $\varepsilon_r'(f)$ curves. The imaginary part of the complex dielectric constant characterizes these losses, and thus the $\varepsilon_r''(f)$ curves have a maximum at the relaxation frequency.

As the frequency is increased still further, the inertial constraints of the dipolar molecules in rotation about their centers of mass is such that no charge displacement occurs at all. The displacement flux from

the rotating dipoles no longer exists, and the remaining lossless interaction consists of the much weaker electronic, and possibly ionic polarization processes. This is why the relative dielectric constant drops from 87.9 to 4.9 for water at 0^{o} C during its dipolar dielectric relaxation. The Debeye equation (shown in Figure A2) models this relaxation process precisely, provided that the necessary parameters, ε'_{ro} and $\varepsilon'_{r\infty}$, can be determined.

It should be mentioned that the process descriptions given in this appendix represent necessary simplifications of the currently accepted conceptual models. The reader who is interested in pursuing the complete story is directed to "Aqueous Dielectrics" by J. B. Hasted (Hasted, 1973).

A.3 Relevance to Microwave Remote Sensing

As pointed out in the thesis text, the fact that the dielectric relaxations of ice and water occur at widely differing frequencies and that the relaxation of water occurs in the microwave region (Figure A2) allows two equations to be written which can be solved for two unknowns (the depth of water and the depth of ice) with the aid of dual-frequency microwave data. This data must be collected in the frequency region where the dielectric relaxation of water occurs, but it is desired to keep the loss tangent $\varepsilon''/\varepsilon'$ to a minimum, because any significant dielectric losses must be accounted for in predicting propagation velocities. Including the loss effects would complicate the analysis such that a simple model, as proposed, would not perform adequately. Also there is a practical limit on the depth

of electromagnetic penetration, which dictates the use of frequencies where the loss tangent is small.

Because the dielectric relaxation of ice occurs in the kilohertz range, the only dielectric losses of interest in an ice, air, and liquid water mixture (snow) are due to the relaxation of liquid water present in the mixture[2]. It is for this reason that the restrictions on liquid water content and operating frequency are placed as limits on the electrical path length dielectric mixture model's generality.

---

[2]It should be pointed out that the conduction process (caused by dissolved ions in the water) dissipates energy in much the same manner as dielectric relaxation does, and this type of loss affects propagation velocities also. However, in natural snowpacks at remote mountain sites the conductivities would usually be so small that they could be neglected.